Studies on molecular determinants for susceptibilities of bats to filoviruses

（フィロウイルスに対するコウモリの感受性を決定する分子基盤に関する研究）

Yoshihiro TAKADATE

Contents

Abbreviations ---------- 1

Preface ---------- 4

Chapter I: Different tropisms between Ebola and Marburg viruses controlled by heterogeneity of bat Niemann-Pick C1 orthologues

Introduction ---------- 7

Materials and Methods ---------- 9

Cells

Viruses

Biosafety

Sequencing of NPC1 genes and plasmid construction

Stable cell lines expressing NPC1 proteins

Solid-phase NPC1-GP binding assay

Molecular modeling

Statistical analysis

Results ---------- 19

Differential susceptibility to EBOV and MARV between bat-derived cell lines FBKT1 and ZFBK13-76E

Rescued susceptibility of FBKT1 and ZFBK13-76E cells expressing exogenous human NPC1

Unique aa sequences found in NPC1 of FBKT1 and ZFBK13-76E cells

Importance of aa residues in NPC1-C loop regions in the cell susceptibility to EBOV and MARV infection

Comparison and identification of aa residues at the GP RBD and NPC1-binding interface

Discussion ---------- 37

Summary ---------- 47

Chapter II: Niemann-Pick C1-mediated distinctive host cell preference of a bat-derived filovirus, Lloviu virus

Introduction ---------- 48

Materials and Methods ---------- 53

Cells

Viruses

Cloning of bat NPC1 genes and generation of stable cell lines expressing chimeric HEK293T/SuBK12-08 NPC1 proteins

Statistical analysis

Results ---------- 51

Susceptibility of bat-derived cell lines to VSV-EBOV, -MARV, and -LLOV

Amino acid sequences of the domain C of bat NPC1 orthologues and susceptibilities of Vero E6 cell lines expressing exogenous NPC1 proteins to VSV-EBOV, -MARV, and -LLOV

Comparison of amino acid sequences at the NPC1-binding interface of filovirus GP and the infectivity of VSV pseudotyped with EBOV, LLOV, and their mutant GPs in SuBK12-08 cells

Discussion ---------- 62

Summary ---------- 65

Conclusion ---------- 66

Acknowledgments ---------- 68

Abstract in Japanese ---------- 71

References ---------- 75

Abbreviations

A	Alanine
BDBV	Bundibugyo virus
BOMV	Bombali virus
BSA	Bovine serum albumin
BSL-4	Biosafety level-4
C	Cysteine
CHAPS	3-([3-Cholamidopropyl] dimethylammonio) propanesulfonate
D	Aspartic acid
DAPI	4',6-diamidino-2-phenylindole, dihydrochloride
dGP	Digested GP
DMEM	Dulbecco's modified Eagle's medium
E	Glutamic acid
E. helvum	*Eidolon helvum*
EBOV	Ebola virus
EDTA	Ethylenediaminetetraacetic acid
ELISA	Enzyme-linked immune sorbent assay
F	Phenylalanine
FCS	Fetal calf serum
FITC	Fluorescein isothiocyanate
G	Glycoprotein of VSV
G	Glycine
GFP	Green fluorescent protein
GP	Glycoprotein of filovirus
H	Histidine
HEK293T	Human embryo kidney 293T
HRP	Horseradish peroxidase
IFN	Interferon
IgG	Immunoglobulin
IU	Infectious unit
K	Lysine

L	Leucine
LAMP1	Lysosomal-associated membrane protein 1
LLOV	Lloviu virus
MARV	Marburg virus
MLAV	Mengla virus
NIH	National Institutes of Health
NP	Nucleoprotein
NPC1	Niemann-Pick C1
NPC1-C	The domain C of Niemann-Pick C1
NPC2	Niemann-Pick C2
OD	Optical density
P	Proline
PBS	Phosphate-buffered saline
P. alecto	*Pteropus alecto*
PBST	Phosphate-buffered saline with Tween 20
PCR	Polymerase chain reaction
PDB	Protein Data Bank
P. vampyrus	*Pteropus vampyrus*
Q	Glutamine
R. aegyptiacus	*Rousettus aegyptiacus*
RAVV	Ravn virus
RBD	Receptor binding domain
RESTV	Reston virus
RPMI	Roswell Park Memorial Institute
S	Serine
SDS	Sodium dodecyl sulfate
sp.	species
SUDV	Sudan virus
T	Threonine
TAFV	Taï Forest virus
$TCID_{50}$	50% tissue culture infectious dose

TMB	3,3’,5,5’-Tetramethyl benzidine
V	Valine
VLP	Virus-like particle
VP	Virus protein
VSV	Vesicular stomatitis virus

Preface

Viruses in the family *Filoviridae* are divided into five genera: *Marburgvirus*, *Ebolavirus*, *Cuevavirus*, *Striavirus*, and *Thamnovirus*. There is one known species in the genus *Marburgvirus*, *Marburg marburgvirus*, consisting of two viruses, Marburg virus (MARV), and Ravn virus (RAVV). There are five distinct species in the genus *Ebolavirus*: *Zaire ebolavirus*, *Sudan ebolavirus*, *Taï Forest ebolavirus*, *Bundibugyo ebolavirus*, and *Reston ebolavirus*, represented by Ebola virus (EBOV), Sudan virus (SUDV), Taï Forest virus (TAFV), Bundibugyo virus (BDBV), and Reston virus (RESTV), respectively[2)]. A novel ebolavirus species, *Bombali ebolavirus*, represented by Bombali virus (BOMV), has been proposed recently[23)]. The genus *Cuevavirus* is made up of a single species, Lloviu virus (LLOV), whose RNA genome was detected in insectivorous bats in Europe[34,57)]. The other two genera, *Striavirus* and *Thamnovirus*, have a single species respectively with viruses whose genomes were detected in fishes in China. Recently, a novel filovirus, Měnglà virus (MLAV), was found in China and a new genus (*Dianlovirus*) has been proposed for this virus[87)]. EBOV, SUDV, TAFV, BDBV, MARV, and RAVV cause severe hemorrhagic fever in humans and nonhuman primates[20)]. Since infectious LLOV, BOMV, and MLAV have never been isolated, nothing is known about the pathogenicity of these viruses in humans and nonhuman primates. Although filovirus diseases in humans have only been reported from central and west African countries[13)], ecological and epidemiological studies strongly suggest the occurrence of unrecognized filovirus infections in humans and animals in nonendemic areas in Africa, and even in Asian and European countries[4,12,22,23,34,52,53,57,61,69,82,87)].

It has been shown that a variety of animal species (e.g., domestic pigs, duikers, dogs, fishes, and bats) were infected with filoviruses. Of these animals, some species of

bats are suspected to be the natural reservoir of filoviruses, which is the species that maintain the infectious virus in nature[65]. Numerous epidemiological studies have suggested that filoviruses infect many bat species, including frugivorous and insectivorous bats, both of which are widely distributed in African, European, and Asian countries[66]. Viral RNA genomes of EBOV, RESTV, BOMV, LLOV, MLAV, MARV, and RAVV have been detected in bats[3,23,29,34,41,57,69,78,83,84,87]. However, infectious ebolaviruses (EBOV, SUDV, TAFV, BDBV, RESTV, and BOMV), LLOV, and MLAV have never been isolated from any species of bats[23,34,41,57,87], while infectious MARV and RAVV were both isolated from a particular fruit bat species (i.e., *Rousettus aegyptiacus* [*R. aegyptiacus*])[3,83]. Interestingly, it has been experimentally demonstrated that MARV, but not ebolaviruses, efficiently infects *R. aegyptiacus* bats and replicates in multiple organs[31], suggesting a difference in host preference between marburgviruses and ebolaviruses. Previous *in vitro* studies also indicate that some bat-derived cell lines have differential susceptibility to each filovirus[28,38,45,60] .

The envelope glycoprotein (GP) is the only viral surface protein of filoviruses, and thus mediates both receptor binding and membrane fusion in the process of viral entry into cells[80]. During the entry step, GP interacts with multiple host molecules. Infection is initiated by the binding of the virus to attachment factors such as C-type lectins[1], and virus particles are then internalized into the host cells *via* micropinocytosis[55,75]. Viral particles are delivered to the late endosome. The low pH environment of the late-endosome leads to the cysteine protease-mediated proteolysis of GP[11]. Then, the digested GP (dGP) interacts with the host endosomal fusion receptor Niemann-Pick C1 (NPC1)[9,15,58], which is a lysosomal cholesterol transporter ubiquitously expressed in many cell types[10,16,17,27]. Loss of NPC1 function is known to cause a fatal

neurodegenerative disorder (i.e., Niemann-Pick disease type C)[10]. The interaction between dGP and NPC1 allows for fusion of the viral envelope and the host endosomal membrane and is hypothesized to be a major determinant in the host range of various filoviruses[35,56,60].

Although bat-derived cell lines have been reported to have different susceptibilities to filoviruses, the underlying molecular mechanisms which determine viral host range remains unclear. I postulated that each viral species has a preferred bat species and sought to identify the biological factors that determine susceptibility of specific bat cells to different filoviruses. In this thesis, I investigated the molecular basis underlying the host range of filoviruses by focusing on the interaction between filovirus GPs and NPC1. In chapter I, I show the molecular determinants for the differential susceptibilities of two cell lines derived from a Yaeyama flying fox (*Pteropus dasymallus yayeyamae*) and a straw-colored fruit bat (*Eidolon helvum* [*E. helvum*]) (i.e., FBKT1 and ZFBK13-76E cells, respectively) to MARV and EBOV, respectively. In chapter II, I demonstrate the mechanisms for the preferential susceptibility of a *Miniopterus* bat (*Miniopterus* sp.)-derived cell line (i.e, SuBK12-08 cells) to LLOV.

Chapter I:

Different tropisms between Ebola and Marburg viruses controlled by heterogeneity of bat Niemann-Pick C1 orthologues

Introduction

It has been suggested that filoviruses have different tropism depending on bat species. Previous studies using vesicular stomatitis virus (VSV) pseudotyped with filovirus GPs demonstrated that FBKT1 cells might be susceptible to EBOV, but not MARV[45], and a straw-colored fruit bat-derived cell line might be susceptible to MARV, but not EBOV[58]. However, the molecular determinants for this differential susceptibility of these bat-derived cell lines to EBOV and MARV remain poorly understood[28,38,45,60]. Thus, in chapter I, I compared the susceptibilities of several bat cell lines derived from various bat species using VSV pseudotyped with filovirus GPs and infectious EBOV and MARV, and found that while most bat-derived cell lines showed some susceptibility to both viruses, FBKT1 was not susceptible to MARV and ZFBK13-76E showed remarkably low susceptibility to EBOV.

The interaction between dGP and NPC1 is thought to be important for filovirus entry into cells. The published co-crystal structures of EBOV dGP and the domain C of human NPC1 (NPC1-C), which is the key region facilitating their interaction demonstrated that there are two surface-exposed loops on NPC1 (i.e., amino acid positions 420-428 and 501-508) which mediate its interactions with dGP[86]. Interestingly, it has been shown that sequence variations in the NPC1-C loops influence the susceptibility of cell lines derived from humans and snakes to filoviruses[35,56], suggesting that the interaction between NPC1 and GP is important for host-range restriction of

filoviruses.

In chapter I, I determined the molecular basis for different susceptibilities of FBKT1 and ZFBK13-76E cells to MARV and EBOV by focusing on the interaction between filovirus GPs and NPC1.

Materials and Methods

Cells

Vero E6 and human embryonic kidney (HEK) 293T cells were grown in Dulbecco's modified Eagle's medium (DMEM) (Sigma) supplemented with 10% fetal calf serum (FCS) (Cell Culture Bioscience), 100 U/ml penicillin, and 0.1 mg/ml streptomycin (Gibco). Bat-derived cell lines were established as described previously[44,45,46,63,77]. All of the bat cell lines were grown in Roswell Park Memorial Institute (RPMI) 1640 medium (Sigma) supplemented with 10% FCS, 100 U/ml penicillin, and 0.1 mg/ml streptomycin. Origins of these cell lines are shown in Table 1.

Viruses

Using VSV containing the green fluorescent protein (GFP) gene instead of the receptor binding VSV glycoprotein (G) gene, pseudotyped viruses with GPs of EBOV (Mayinga), SUDV (Boniface), TAFV (Pauléoula), BDBV (Butalya), RESTV (Pennsylvania), and MARV (Angola) were generated as described previously[14,80]. The amounts of GPs incorporated into VSV particles were measured by western blotting with a mixture of a rabbit anti-BDBV GP antiserum (FS0510), which is produced by immunization with a synthetic peptide corresponding to amino acid residues 83–97 (TKRWGFRAGVPPKVV) of BDBV GP, and a mouse anti-MARV GP monoclonal antibody (AGP127-8)[32] and confirmed to be similar among virus species (data not shown). Mutant GP genes were constructed by site-directed mutagenesis and were cloned into the protein expression vector pCAGGS[62]. VSVs pseudotyped with filovirus GPs (VSV-EBOV, -SUDV, -TAFV, -BDBV, -RESTV, and -MARV) were preincubated with

Table 1. Origins of cell lines used in this study

Cell line	Common name	Scientific name[a]	Organ
Vero E6	African green monkey	*Chlorocebus* sp.	Kidney
HEK293T	Human	*Homo sapiens*	Kidney
FBKT1	Yaeyama flying fox	*Pteropus dasymallus yayeyamae*	Kidney
ZFBK13-76E	Straw-colored fruit bat	*Eidolon helvum*	Kidney
ZFBK11-97	Peter's epauletted fruit bat[b]	*Epomophorus crypturus*	Kidney
ZFBK15-137RA	Egyptian fruit bat	*Rousettus aegyptiacus*	Kidney
DemKT1	Leschenault's rousettes	*Rousettus leschenaultii*	Kidney
SuBK12-08	The long-fingered bat[c]	*Miniopterus* sp.	Kidney
YubFKT1	Eastern bent-winged bat	*Miniopterus fuliginosus*	Kidney
BKT1	Greater horseshoe bat	*Rhinolophus ferrumequinum*	Kidney

[a]Scientific names of the species are shown in italic. [b]Temporarily identified by habitat and nucleotide sequence of cytochrome *b* genes (97% in BLAST search). The East African epauletted fruit bat (*Epomophorus minimus*), Ansell's epauletted fruit bat (*Epomophorus anselli*), Peter's dwarf epauletted fruit bat (*Micropteropus pusillus*) and Gambian epauletted fruit bat (*Epomophorus gambianus*) are also genetically similar (97%). [c]Temporarily identified by habitat and nucleotide sequence of cytochrome *b* genes (99% in BLAST search).

the anti-VSV G monoclonal antibody VSV-G [N] 1-9[54] to abolish the background infectivity of parental VSV. Tenfold diluted pseudotyped VSVs were inoculated onto confluent cell monolayers cultured on 96-well plates, and the infectious unit (IU) in each cell line was determined twenty hours later by counting the number of GFP-expressing cells under a fluorescent microscope. Relative infectivity of pseudotyped VSVs in an NPC1-knockout Vero E6 cell line (Vero E6/NPC1-KO cl.19) expressing exogenous NPC1 was determined by setting the GFP-positive cell number of wildtype HEK293T-NPC1-expressing cells infected with each virus to 100%.

Infectious EBOV (Mayinga) and MARV (Musoke) were used for titration in Vero E6, FBKT1, ZFBK13-76E, and DemKT1 cells. Tenfold diluted stock viruses were inoculated onto cell lines in 96-well plates. Cells were fixed with 10% formalin 3 days postinfection and stained with a mixture of a mouse anti-EBOV GP monoclonal antibody (ZGP42/3.7)[21] and a mouse anti-EBOV nucleoprotein (NP) monoclonal antibody (ZNP74-7)[14] or a mixture of a rabbit anti-MARV GP and NP antisera (FS0505 and FS0608, respectively)[21] as primary antibodies, and anti-mouse immunoglobulin G (IgG) (Jackson ImmunoResearch, 115-095-003) or anti-rabbit IgG (Jackson ImmunoResearch, 711-096-152) conjugated with fluorescein isothiocyanate (FITC) as secondary antibodies. Infected cells were observed under a fluorescent microscope. 50% tissue culture infectious dose ($TCID_{50}$) values were calculated by the Reed and Muench method.

Infectious EBOV-GFP (Mayinga)[18] and MARV (Angola) were used for focus-forming assays as described previously[32,35]. These infectious filoviruses were inoculated onto confluent cell monolayers cultured in 96-well plates. After adsorption for 1 hour, the inoculum was replaced with Eagle's minimal essential medium containing 1.2% carboxymethyl cellulose. After incubation for 3 days, cells were fixed. MARV-infected

cells were immunostained with a mixture of rabbit anti-MARV GP and NP (FS0505 and FS0609, respectively)[21] as primary antibodies followed by anti-rabbit IgG conjugated with Alexa Fluor 488 (A11034, Invitrogen) as a secondary antibody. Focus-forming units of filoviruses were quantified by counting the number of fluorescent foci. Relative infectivity was determined by setting focus forming unit values given by Vero E6 cells expressing wildtype HEK293T-NPC1 to 100%.

Biosafety

Infectious work with wildtype EBOV and MARV was performed in the Galveston National Laboratory biosafety level 4 (BSL-4) laboratory at the University of Texas Medical Branch and in the BSL-4 laboratory at the Integrated Research Facility of the Rocky Mountain Laboratories, Division of Intramural Research, National Institute of Allergy and Infectious Diseases, National Institutes of Health (NIH; Hamilton, MT). Experiments were performed following the standard operating procedures approved by the Institutional Biosafety Committees.

Sequencing of NPC1 genes and plasmid construction

Total RNA was extracted from FBKT1, ZFBK13-76E, ZFBK11-97, ZFBK15-137RA, DemKT1, SuBK12-08, YubFKT1, and BKT1 cells using ISOGEN (Nippongene) and mRNAs were reverse transcribed with Superscript IV (Invitrogen). To amplify NPC1 genes of FBKT1 and ZFBK13-76E, polymerase chain reaction (PCR) was performed with KOD-Plus Neo (TOYOBO) using primer sets designed based on the sequences of *Pteropus vampyrus* (*P. vampyrus*) (GenBank accession number; XM_023530841.1) and *Miniopterus natalensis* bats (GenBank accession number; XM_016211523.1). PCR

products were directly sequenced or cloned into TOPO (Invitrogen) or pSP72 (Promega) plasmid vectors followed by sequencing. After sequence confirmation, wildtype and mutant NPC1 genes of HEK293T, FBKT1, and ZFBK13-76E were inserted into the pMXs-puro retroviral vector (Cell Biolabs). The plasmids of mutant NPC1 genes were constructed by site-directed mutagenesis with KOD-Plus Neo. After sequence confirmation, these mutant genes were inserted into the retroviral vector. An In-Fusion cloning kit (BD Clontech) was used for constructing the retroviral vectors carrying NPC1 genes. All NPC1 sequences of FBKT1, ZFBK13-76E, ZFBK11-97, ZFBK15-137RA, DemKT1, SuBK12-08, YubFKT1, and BKT1 have been deposited in GenBank under ID codes LC462999, LC462993, LC462994, LC462995, LC462996, LC462997, LC462271, and LC462998, respectively.

Establishment of Vero E6/NPC1-KO cell line

Vero E6/NPC1-KO cells were previously generated in this laboratory[35]. Briefly, guide RNA (gRNA) sequences were designed by using CRISPRdirect web tool (https://crispr.dbcls.jp/). Synthesis of the gRNA template, *in vitro* transcription of g RNA, and purification of gRNA were performed by using GeneArt precision gRNA synthesis kit (Invitrogen). Vero E6 cells were transfected with the mixture of gRNA products and Platinum Cas9 nuclease (Invitrogen), using Lipofectamine CRISPRMAX Cas9 Transfection Reagent (Invitrogen). Three days post transfection, the presence of genomic cleavage was confirmed by using a GeneArt Genomic Cleavage Detection Kit (Invitrogen) (data not shown). After the clonal expression of these cell for three weeks, deletion of NPC1 protein expression was confirmed by Western blotting (data not shown).

Stable cell lines expressing NPC1 proteins

To generate retroviruses carrying NPC1 genes, HEK293T-derived Platinum-GP cells (Cell Biolabs) were co-transfected with pMXs-puro encoding NPC1 genes and the expression plasmid pCAGGS encoding the VSV G using Lipofectamine 2000 (Invitrogen). Empty pMXs-puro was used for vector control cells. Forty-eight hours later, the culture supernatants containing retroviruses were collected, filtered through 0.45-μm filters, and used to infect FBKT1, ZFBK13-76E, and Vero E6/NPC1-KO cl.19. Transduced cells stably expressing exogenous NPC1 were selected with a growth medium, containing 6.0 μg/ml (FBKT1), 1.0 μg/ml (ZFBK13-76E), or 10.0 μg/ml (Vero E6/NPC1-KO cl.19) puromycin (Sigma-Aldrich). I examined expression levels and intracellular localization of exogenous NPC1 molecules in western blotting and confocal microscopy and confirmed that similar band intensities and lysosomal localization were uniformly observed in each cell line (Figure 1). I also confirmed the expression of human NPC1 protein in HEK293T NPC1 transduced bat cell lines (data not shown).

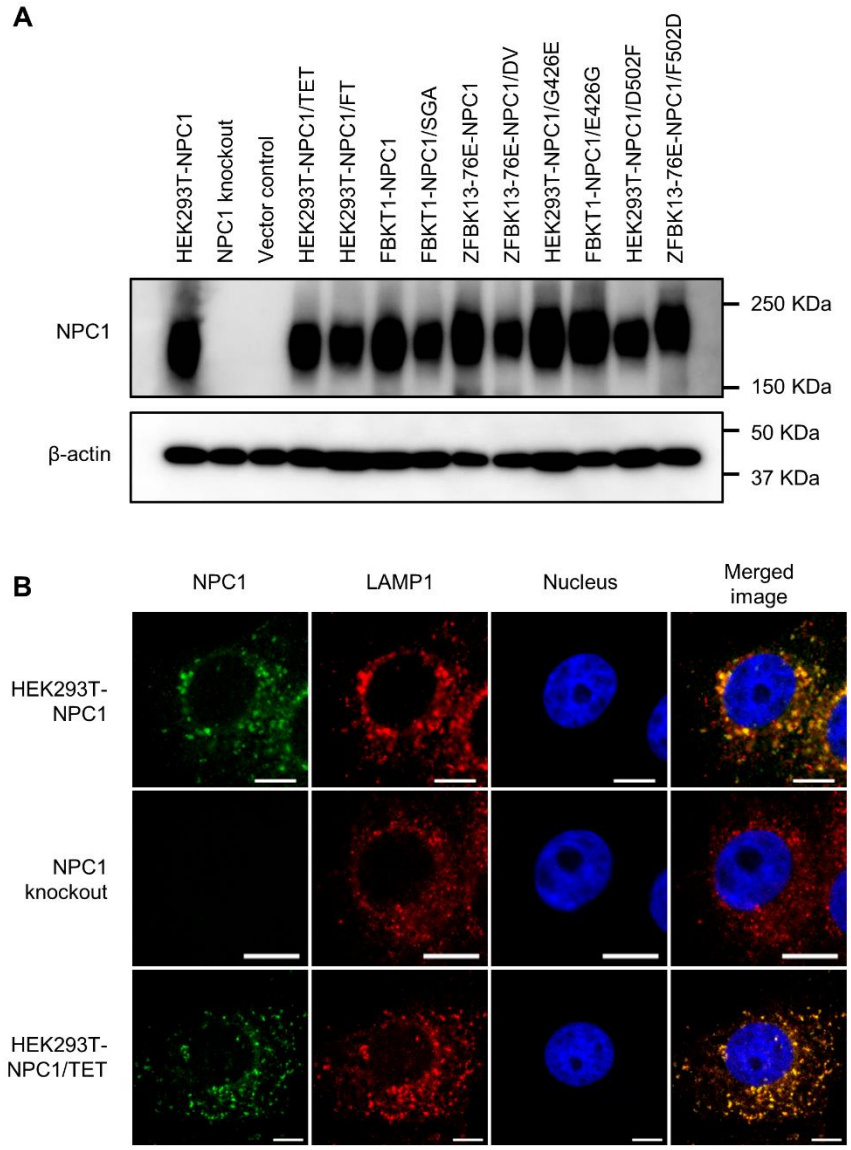

Figure 1. Expression of exogenous NPC1 in Vero E6/NPC1-KO cl.19 cells

(A) Western blotting for wildtype and mutant NPC1 expression. Each cell lysate was subjected to sodium dodecyl sulfate (SDS)-polyacrylamide gel electrophoresis followed by western blotting with rabbit anti-NPC1 monoclonal antibody (ab134113, Abcam), mouse anti-β actin monoclonal antibody (ab6276, Abcam), HRP-conjugated goat anti-rabbit IgG (074-1506, KPL), and HRP-conjugated goat anti-mouse IgG (115-035-062, Jackson ImmunoResearch). The bound antibodies were visualized with Immobilon Western (Millipore). (B) Co-localization of NPC1 and a lysosome marker, Lysosomal-associated membrane protein 1 (LAMP1). Representative cell images are shown here. Cells were grown in Millicell EZ SLIDE 8-well glass (Millipore). NPC1 was stained with

rabbit anti-NPC1 monoclonal antibody (ab134113, Abcam) and donkey anti-rabbit IgG (H+L) antibodies conjugated with Alexa Fluor 488 (A21206, Invitrogen). Anti-LAMP1 antibodies (SAB3500285, Sigma-Aldrich) were conjugated with Alexa Fluor 594 using APEX Alexa Fluor 594 Antibody Labelling (ab134113, Abcam) and donkey anti-rabbit IgG (H+L) antibodies conjugated with Alexa Fluor 488 (A21206, Invitrogen). Anti-LAMP1 antibodies (SAB3500285, Sigma-Aldrich) were conjugated with Alexa Fluor 594 using APEX Alexa Fluor 594 Antibody Labelling Kit (Invitrogen) and then used. The nucleus was stained using 4',6-diamidino-2-phenylindole, dihydrochloride (DAPI) (Molecular Probes). Images were taken with 63x oil immersion objective on a Zeiss LSM 780 confocal laser microscope and analyzed with ZEN 2.3 Lite software. The expression of NPC1 (green), LAMP1 (red), and nucleus (blue) are shown separately or as merged images. The scale bars represent 10 μm.

Solid-phase NPC1-GP binding assay

Vero E6/NPC1-KO cells and Vero E6/NPC1-KO cells expressing HA-tagged NPC1 and its mutants[35] were lysed with CHAPS-NTE buffer (0.5% wt/vol CHAPS [3-[[3-Cholamidopropyl]dimethylammonio]propanesulfonate], 140 mM NaC1, 10 mM Tris-HC1, 1 mM EDTA [Ethylenediaminetetraacetic acid]; pH7.5) (10^7 cells/ml). Then, EDTA-free Complete Protease Inhibitor Cocktail (Roche) was added. The cells were sedimented at 10,000 × *g* for 10 min at 4˚C, and the supernatant was harvested. Virus-like particles (VLPs) (4-6 mg/ml in phosphate-buffered saline [PBS]) were treated with thermolysin (Sigma) at 37˚C for 90 min. The VLP solution was diluted at 1:10 with 0.05 M carbonate buffer (pH9.6). Enzyme-linked immune sorbent assay (ELISA) plates (Maxisorp, Nunc) were coated with the diluted VLPs, and incubated at 4˚C overnight. The VLPs were removed and the plates were blocked with bovine serum albumin (BSA) (10 mg/ml in PBS) and incubated at room temperature for 2 hours. After washing the plates once with 0.05% Tween 20 in PBS (PBST), the cell lysate was added to each well and incubated at 4˚C overnight. After removal of the lysate, the plates were washed with PBST 3 times, and rat anti-HA antibody 3F10 (Sigma) diluted with PBST containing BSA (5 mg/ml) was added, and then incubated at room temperature for 1 hour. After washing 3 times with PBST, horseradish peroxidase (HRP)-conjugated anti-rat IgG (H+L) (Jackson ImmunoResearch) was added to each well. After incubation at room temperature for 1 hour, the plates were washed 4 times with PBST and the 3,3',5,5'-Tetramethyl-benzidine (TMB) substrate (Sigma) was added and incubated in the dark at room temperature for 60 min. The optical density (OD) value at 450 nm was measured after stopping the reaction with 1M phosphoric acid.

Molecular modeling

Three-dimensional models of the NPC1-C and EBOV GP complex were prepared based on a previous study[86] (Protein Data Bank [PDB] code 5F1B). Three-dimensional structures shown in the figures of this study were prepared using PyMOL (Schrödinger LLC).

Quantification and statistical analysis

All statistical analyses were performed using R software (version 3.5.2)[71]. For comparison of viral infectivity between NPC1-transduced cell lines, reported in Figure 5 and Figure 10, one-way analysis of variance, was performed, followed by Dunnett's test. Student *t*-test was used in Figure 8. *P*-values of less than 0.05 were considered to be significant.

Results

Differential susceptibility to EBOV and MARV between bat-derived cell lines FBKT1 and ZFBK13-76E

Using non-replicating VSVs pseudotyped with GPs of EBOV, SUDV, TAFV, BDBV, RESTV, and MARV (VSV-EBOV, -SUDV, -TAFV, -BDBV, -RESTV, and -MARV, respectively), I investigated GP-dependent tropism, which appears to be the principal determinant for the host range-restriction of filoviruses. Vero E6 cells, which are commonly used for filovirus studies, HEK293T cells, and eight bat-derived cell lines of different origins were used to compare their susceptibilities (Table 1 and Figure 2)[44,45,46,63,77]. I found that Vero E6, HEK293T, and the bat-derived cell lines, except FBKT1 and ZFBK13-76E, were susceptible to all pseudotyped VSVs tested. Consistent with a previous study[45], FBKT1 was susceptible to VSV-EBOV, -SUDV, -TAFV, -BDBV, and -RESTV, but not to VSV-MARV. In contrast, ZFBK13-76E was susceptible to VSV-SUDV, -TAFV, -BDBV, -RESTV, and -MARV, but not to VSV-EBOV, indicating that cell lines derived from this bat species might be less susceptible to EBOV[60]. Next, the impaired GP-dependent susceptibilities of FBKT1 and ZFBK13-76E were confirmed using infectious filoviruses (Table 2). Consistent with the results for pseudotyped VSVs, FBKT1 cells showed susceptibility to infectious EBOV but not to MARV. Although ZFBK13-76E cells were susceptible to both EBOV and MARV, the infectivity of EBOV in ZFBK13-76E cells was significantly lower than in Vero E6, FBKT1, and DemKT1 cells.

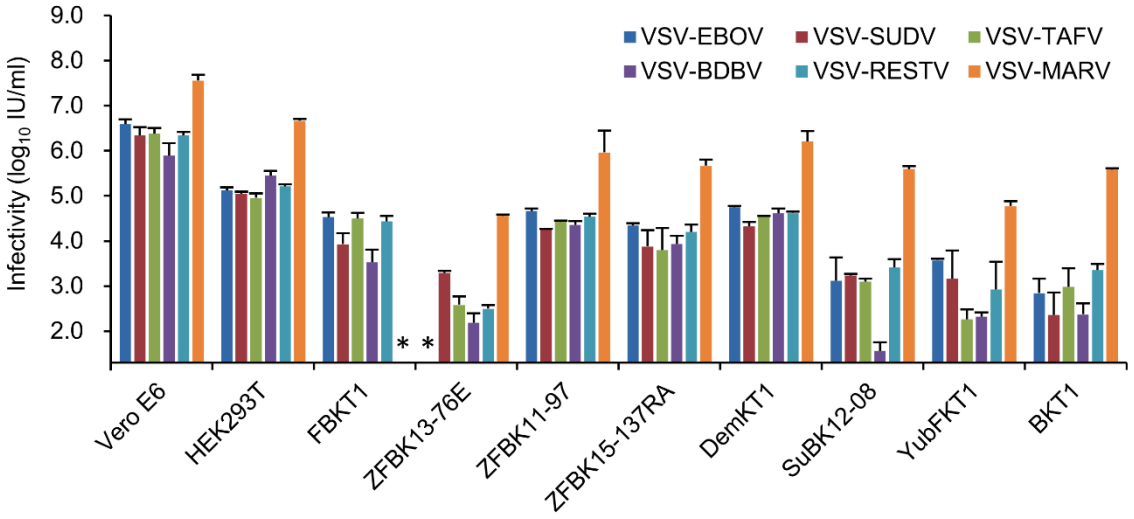

Figure 2. Susceptibility of cell lines to VSVs pseudotyped with filovirus GPs

Vero E6, HEK293T, and bat-derived cells were infected with VSVs pseudotyped with filovirus GPs (VSV-EBOV, -SUDV, -TAFV, -BDBV, -RESTV, and -MARV). Viral IUs in each cell line were determined by counting the number of GFP-expressing cells as described in Materials and Methods. Each experiment was conducted three times, and average and standard deviations are shown. Asterisks represent IUs under the limit of detection (20 IU/ml).

Table 2. Susceptibility of bat-derived cell lines to Ebola (EBOV) and Marburg virus (MARV) infection

Cell lines	Infectivity ($TCID_{50}$/100 µl) [a]		Relative infectivity to Vero E6	
	EBOV	MARV	EBOV	MARV
Vero E6	3.16×10^4	5.01×10^5	1.00	1.00
FBKT1	5.01×10^3	Not detected[b]	0.16	-
ZFBK13-76E	3.16×10^2	2.00×10^5	0.01	0.40
DemKT1	3.16×10^4	3.16×10^5	1.00	0.63

[a]Viral titers in Vero E6 and bat-derived cell lines were determined as the 50% tissue culture infectious dose ($TCID_{50}$).

[b]Infectivity of MARV in FBKT1 cells was under the limit of detection (3.16 $TCID_{50}$/100 µl).

Rescued susceptibility of FBKT1 and ZFBK13-76E cells expressing exogenous human NPC1

Since pseudotyped VSVs rely on GP-dependent entry into cells, the interaction between GP and its ligands is likely the crucial step involved in the differential susceptibility of FBKT1 and ZFBK13-76E cells. Thus, I hypothesized that the impaired susceptibility of FBKT1 and ZFBK13-76E cells to particular filoviruses was due to the structural difference of cellular molecules required for filovirus entry into cells and focused on the interaction between GP and the NPC1 receptor. Although several cellular molecules have been identified as filovirus receptors, the NPC1 molecule is thought to be the only essential receptor required for membrane fusion during filovirus entry into cells[9,15,58]. To investigate whether introduction of human NPC1 affected the susceptibilities of these bat cells, I generated FBKT1 and ZFBK13-76E cells stably expressing exogenous NPC1 derived from HEK293T and infected them with pseudotyped VSVs (Figure 3). As expected, both FBKT1 and ZFBK13-76E became fully susceptible to all of the pseudotyped VSVs upon the expression of the human NPC1. These data indicated that the heterogeneity of NPC1 molecules among FBKT1, ZFBK13-76E, and HEK293T cells was likely involved in the host specificity of MARV and EBOV.

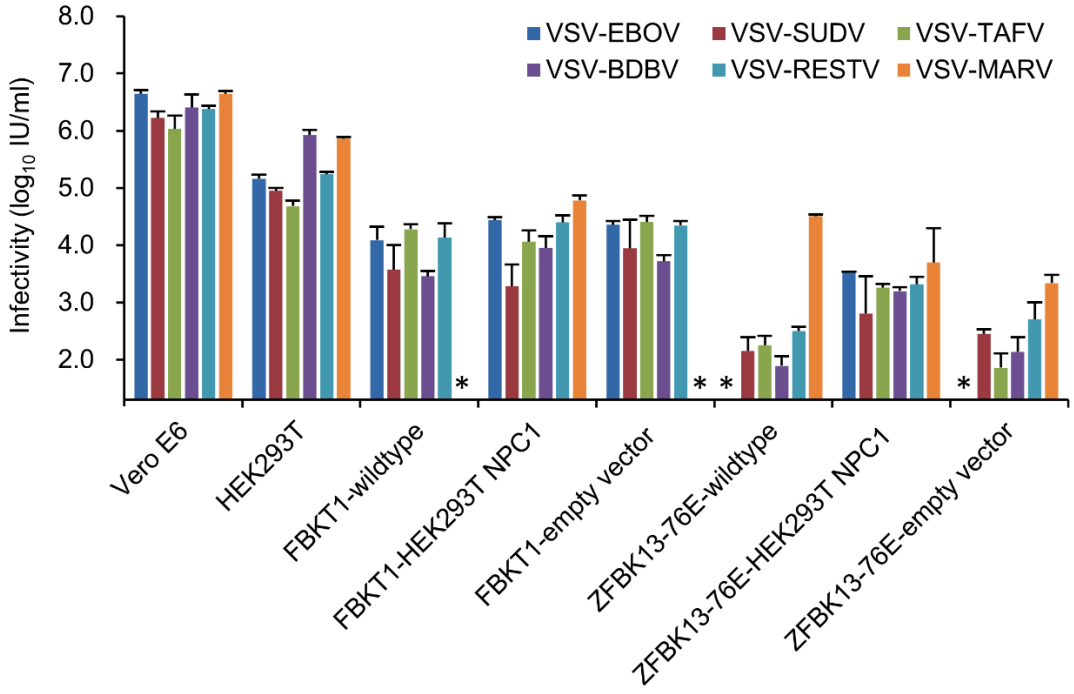

Figure 3. Susceptibility of cell lines to VSVs pseudotyped with filovirus GPs

Vero E6, HEK293T, bat cells (FBKT1 and ZFBK13-76E) expressing exogenous human NPC1, and empty vector-transduced FBKT1 and ZFBK13-76E were infected with VSVs pseudotyped with filovirus GPs. Viral IUs in each cell line were determined by counting the number of GFP-expressing cells as described in Materials and Methods. Each experiment was conducted three times, and average and standard deviations are shown. Asterisks represent IUs under the limit of detection (20 IU/ml).

Unique amino acid sequences found in NPC1 of FBKT1 and ZFBK13-76E cells

Previously published structural data have shown that some of the amino acid residues in loop 1 and loop 2 of the NPC1-C interact with the receptor binding domain (RBD) of EBOV GP (Figure 4A)[24,86]. Thus, I assumed that the loop regions of NPC1-C might have genetic variations that affect susceptibility of FBKT1 and ZFBK13-76E cells to MARV and EBOV infection, respectively. Therefore, I sequenced the NPC1 genes of the bat cell lines and compared the deduced amino acid sequences of the loop regions of bat NPC1 orthologues (Figure 4B). I found that NPC1 proteins of FBKT1 and ZFBK13-76E cells had unique amino acid sequences; FBKT1 cells with threonine (T), glutamic acid (E), and T at positions 425, 426, and 427, respectively, in loop 1 and ZFBK13-76E cells with phenylalanine (F) and T at positions 502 and 505, respectively, in loop 2, whereas the corresponding amino acid residues of HEK293T and Vero E6 cells were serine (S), glycine (G), and alanine (A), in loop 1 and aspartic acid (D) and valine (V) in loop 2. Among the other bat cell lines examined, shared sequences (AGS or SGS in loop 1 and D and V in loop 2) were found.

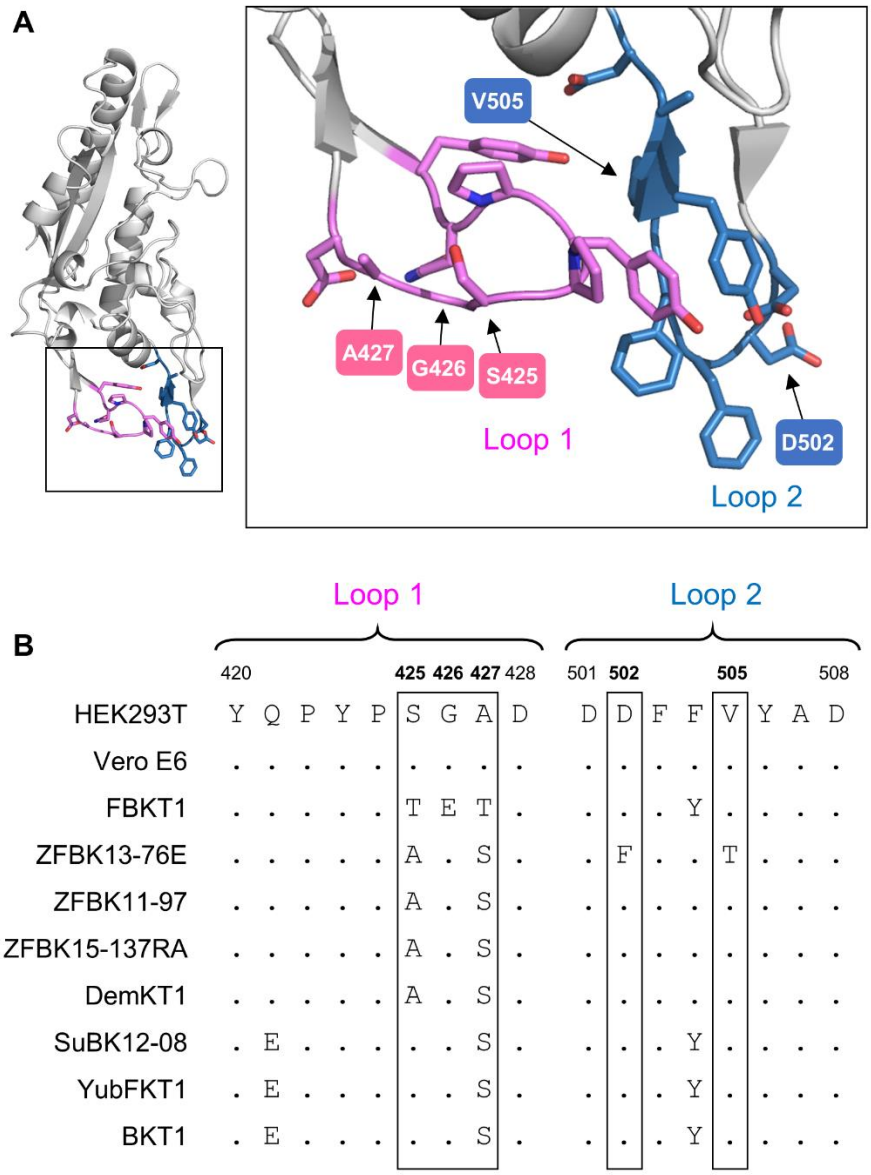

Figure 4. Comparison of amino acid sequences of the domain C loops of bat NPC1 orthologues

(A) The three-dimensional structure of domain C of human NPC1 (PDB ID: 5F1B) is represented as a ribbon model. GP-interacting regions, loop 1 and loop 2 (indicated in violet and sky blue, respectively), are shown in the boxed regions. Nitrogen and oxygen atoms in side chains are shown in blue and red, respectively. (B) Deduced amino acid sequences of the domain C loop regions of NPC1 orthologues are aligned. The amino acid positions including the unique amino acid residues observed in FBKT1 (positions 425, 426, and 427 in the loop 1 region) and ZFBK13-76E (positions 502 and 505 in the loop 2 region) are enclosed by rectangles.

Importance of amino acid residues in NPC1-C loop regions in the cell susceptibility to EBOV and MARV infection

To elucidate the importance of these unique amino acid residues found in the NPC1-C loop regions of FBKT1 and ZFBK13-76E cells, I generated wildtype and NPC1 mutants in which amino acid residues at positions 425, 426, and 427 in loop 1 were swapped between HEK293T and FBKT1 cells and those at positions 502 and 505 in loop 2 were swapped between HEK293T and ZFBK13-76E cells (Figure 5A, B). Then I generated Vero E6 cells stably expressing these exogenous NPC1 molecules using an NPC1-knockout cell line, Vero E6/NPC1-KO cl.19[35], and compared their susceptibilities to VSVs pseudotyped with filovirus GPs (Figure 5C). I observed significantly lower infectivity of VSV-MARV in Vero E6 cells expressing wildtype FBKT1 NPC1 or human NPC1 having 3 point mutations in loop 1 (HEK293T-NPC1/TET) than in those expressing wildtype human NPC1 (HEK293T-NPC1). Interestingly, converse mutations in FBKT1 NPC1 (FBKT1-NPC1/SGA) significantly increased the infectivity of VSV-MARV. In contrast, these mutations did not affect the infection with VSVs pseudotyped with ebolavirus GPs. I also found that expression of wildtype ZFBK13-76E NPC1 (ZFBK13-76E-NPC1) or human NPC1 having 2 point mutations at positions 502 and 505 (HEK293T-NPC1/FT) resulted in significantly lower infectivity of VSV-EBOV than in wildtype human NPC1 and that F502D and T505V mutations in ZFBK13-76E NPC1 (ZFBK13-76E-NPC1/DV) converted the NPC1 function to efficiently mediate VSV-EBOV infection. No significant differences were observed in the infectivity of the other viruses except VSV-TAFV.

These changes of cell susceptibility were confirmed using infectious EBOV and MARV (Figure 5D). Although the infectivity of EBOV in cells expressing wildtype

FBKT1 NPC1 was lower than in those expressing wildtype human NPC1, the reduction was much more prominent in MARV infection. Taken together, these data suggested that the unique amino acid residues found in loop 1 and loop 2 in NPC1-C were major determinants for the differential susceptibility of FBKT1 and ZFBK13-76E cells to EBOV and MARV infection.

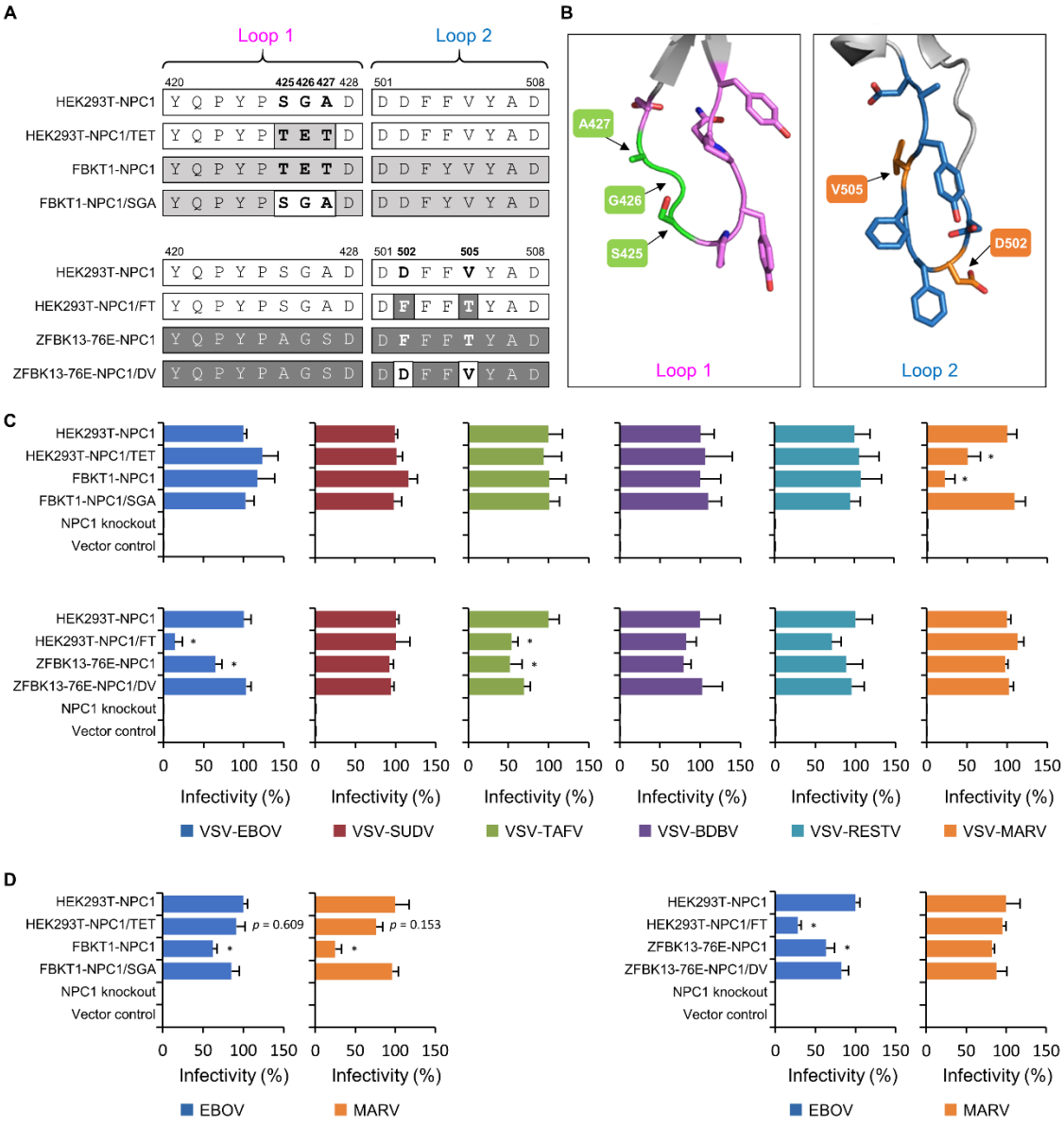

Figure 5. Effects of amino acid substitutions in the NPC1-C loops on cell susceptibility to pseudotyped VSVs, EBOV, and MARV

(A) Wildtype and mutant NPC1 genes were constructed to assess the importance of the unique amino acid sequences (shown in boldface) in loop 1 of FBKT1 and loop 2 of ZFBK13-76E. (B) Locations of the unique amino acid residues of the loop regions are indicated in light green (loop 1) and orange (loop 2). Nitrogen and oxygen atoms in side chains are shown in blue and red, respectively. (C, D) Vero E6/NPC1-KO cl.19 cells transduced with exogenous NPC1 genes and control cells (NPC1 knockout and Vector control) were infected with pseudotyped VSVs (C) or infectious filoviruses (D). Relative infectivity was determined as described in Materials and Methods. Each experiment was

conducted three times (C) or in triplicate (D), and averages and standard deviations are shown. For comparison of viral infectivity among NPC1-expressing cells, one-way analysis of variance was performed, followed by Dunnett's test, and significant differences compared to cells expressing wildtype human NPC1 (HEK293T-NPC1) are shown with asterisks (* $P < 0.05$).

Comparison and identification of amino acid residues at the GP RBD and NPC1-binding interface

The previously determined co-crystal structure of human NPC1-C and EBOV GP has demonstrated that the GP RBD contains key amino acid residues that directly interact with some of the amino acid residues identified above in the loop structures of NPC1-C. Particularly, it has been shown that the identified amino acid motif in loop 1 (i.e., SGA in human NPC1) principally interacts with S at position 142 of GP, and that D at position 502 in loop 2 interacts with cysteine (C) at position 147 of GP[86] (Figure 6A, B). I then compared amino acid sequences around this region of GP (i.e., positions 141-150; EBOV numbering) among all filovirus GPs (Figure 6C) and found an amino acid difference at position 142 (EBOV numbering); S in EBOV, TAFV, and BDBV GPs, and glutamine (Q) in SUDV, RESTV, and MARV GPs at the corresponding amino acid positions. An amino acid difference (C in EBOV, SUDV, TAFV, BDBV, and RESTV GPs, and Histidine [H] in MARV GP) was also found at position 147 (EBOV numbering).

To identify key amino acid residues on RBD for the ability to infect FBKT1 and ZFBK13-76E cells, I generated VSVs pseudotyped with GP mutants whose amino acid at positions 142 (142 for EBOV, SUDV, TAFV, and BDBV, 143 for RESTV, and 126 for MARV) or 147 (147 for EBOV, SUDV, TAFV, and BDBV, 148 for RESTV, and 131 for MARV) were substituted and their IUs were compared using Vero E6, FBKT1, and ZFBK13-76E cells. Though there was no significant difference among the viruses for the infectivity in Vero E6 cells, VSV-EBOV S142Q failed to infect FBKT1 cells, like VSV-MARV, and VSV-MARV Q126S infected FBKT1 cells at a similar extent to VSV-EBOV (Figure 6D). I tested the other amino acid differences between MARV and EBOV GPs at the positions that were suggested to potentially interact with NPC1-C[86], and found that

some of the amino acid substitutions (e.g., V79P, I113V, K114T, and V141I) also reduced the infectivity of VSV-EBOV in FBKT1 but none of them resulted in complete loss of the infectivity and that the A71G substitution altered the infectivity of VSV-MARV in this cell line (Figure 7).VSV pseudotyped with SUDV, TAFV, BDBV, RESTV, and their GP mutants similarly infected FBKT1 cells. Unexpectedly, VSVs pseudotyped with the EBOV GP C147H mutant lacked the ability to infect Vero E6 and ZFBK13-76E cells (data not shown). Since C147 of EBOV GP has been reported to be important for the folding of the GP structure[30], the lack of infectivity was likely due to structural misfolding of the GP molecule. I then focused on the amino acid residue at position 148 (148 for EBOV, SUDV, TAFV, and BDBV, 149 for RESTV, and 132 for MARV), which was assumed to be potentially involved in the interaction between GP and NPC1-C loop 2 based on the co-crystal structures of these molecules (Figure 6E). I indeed found amino acid differences at this position among the viruses (Figure 6C). Thus, I generated VSVs pseudotyped with GPs whose amino acid at this position were substituted and compared their infectivity in Vero E6 and ZFBK13-76E cells (Figure 6E). VSV pseudotyped with the A148P GP mutant of EBOV successfully infected ZFBK13-76E cells as well as VSV-SUDV and -RESTV. The other amino acid substitutions at the positions potentially interacting with NPC1-C[86] showed limited effects to change the infectivity of VSV-MARV to ZFBK13-76E cells (Figure 7). Interestingly, the P148A mutation did not affect the infectivity of VSV pseudotyped with the SUDV GP mutant, whereas VSV-TAFV and -BDBV P148A GP mutants failed to infect ZFBK13-76E cells similarly to VSV pseudotyped with wildtype EBOV GP (Figure 6E). Altogether, these results suggested that Q126 of MARV GP and A148 of EBOV GP were responsible for the reduced ability of MARV and EBOV to infect FBKT1 and ZFBK13-76E cells, respectively.

Finally, binding activities to FBKT1, ZFBK13-76E, and their mutant NPC1 molecules were compared among EBOV and MARV wildtype and mutant GPs (Figure 8). I found that the amino acid substitution of S142Q of EBOV GP reduced the binding activity to FBKT1-NPC1 and HEK293T-NPC1/TET and that the corresponding amino acid substitution (Q126S) of MARV GP enhanced the binding activity to these NPC1 molecules. No significant difference was found in the binding activities to FBKT1-NPC1/SGA between wildtype and mutant GPs of both viruses. Similarly, the A148P substitution of EBOV GP enhanced the binding activity to ZFBK13-76E-NPC1 and HEK293T-NPC1/FT and that no significant difference was found in the binding activities to ZFBK13-76E-NPC1/DV between wildtype and mutant GPs of both viruses.

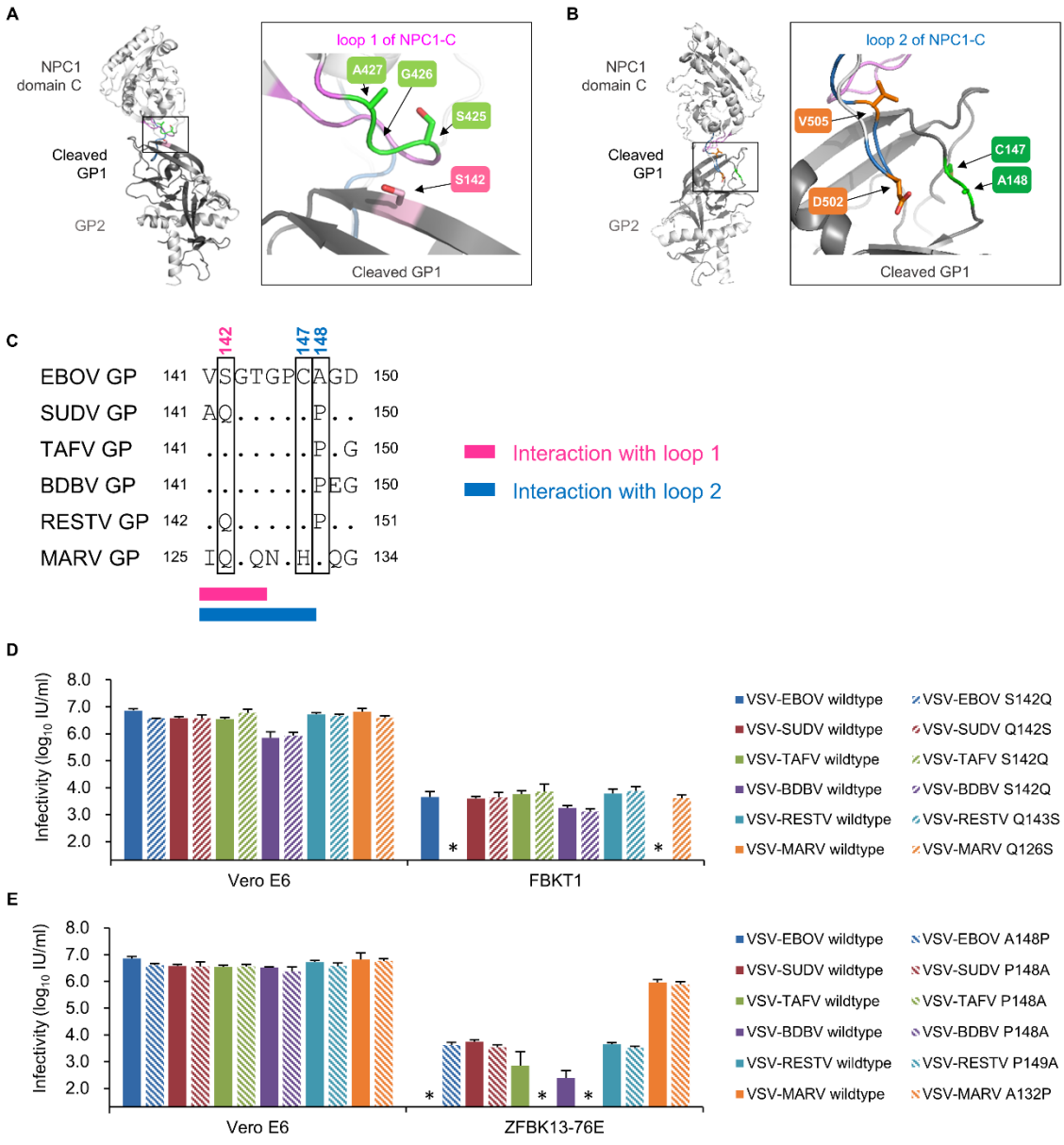

Figure 6. Effects of amino acid substitutions in the GP RBD on the infectivity of pseudotyped VSVs in FBKT1 and ZFBK13-76E cells

(A, B) In the three-dimensional structure of the complex of EBOV GP and human NPC1-C, the GP-NPC1 interfaces are indicated in the boxed regions. The amino acid residues at positions 425-427 (S, G, and A) in NPC1-C loop 1 and at position 142 (S) of EBOV GP are shown in light green and pink, respectively (A). The amino acid residues at positions 502 and 505 (D and V) in NPC1-C loop 2 and at positions 147 and 148 (C and A) of EBOV GP are shown in orange and green, respectively (B). Oxygen atoms in side chains are shown in red (A, B). (C) Deduced amino acid sequences of filovirus GPs are

aligned. The amino acid residues at positions 142 and 147/148, which are assumed to interact with the amino acid at positions at 425-427 in loop 1 and at 502 and 505 in loop 2 of human NPC1-C, respectively, are enclosed by rectangles. (D, E) Vero E6, FBKT1, and ZFBK13-76E cells were infected with VSVs pseudotyped with wildtype and mutant GPs of EBOV, SUDV, TAFV, BDBV, RESTV, and MARV, whose amino acid at positions 142 (D) or 148 (E) were substituted (EBOV numbering). Viral IUs in each cell line were determined by counting the number of GFP-expressing cells. Each experiment was conducted three times, and averages and standard deviations are shown. Asterisks represent IUs under the limit of detection (20 IU/ml).

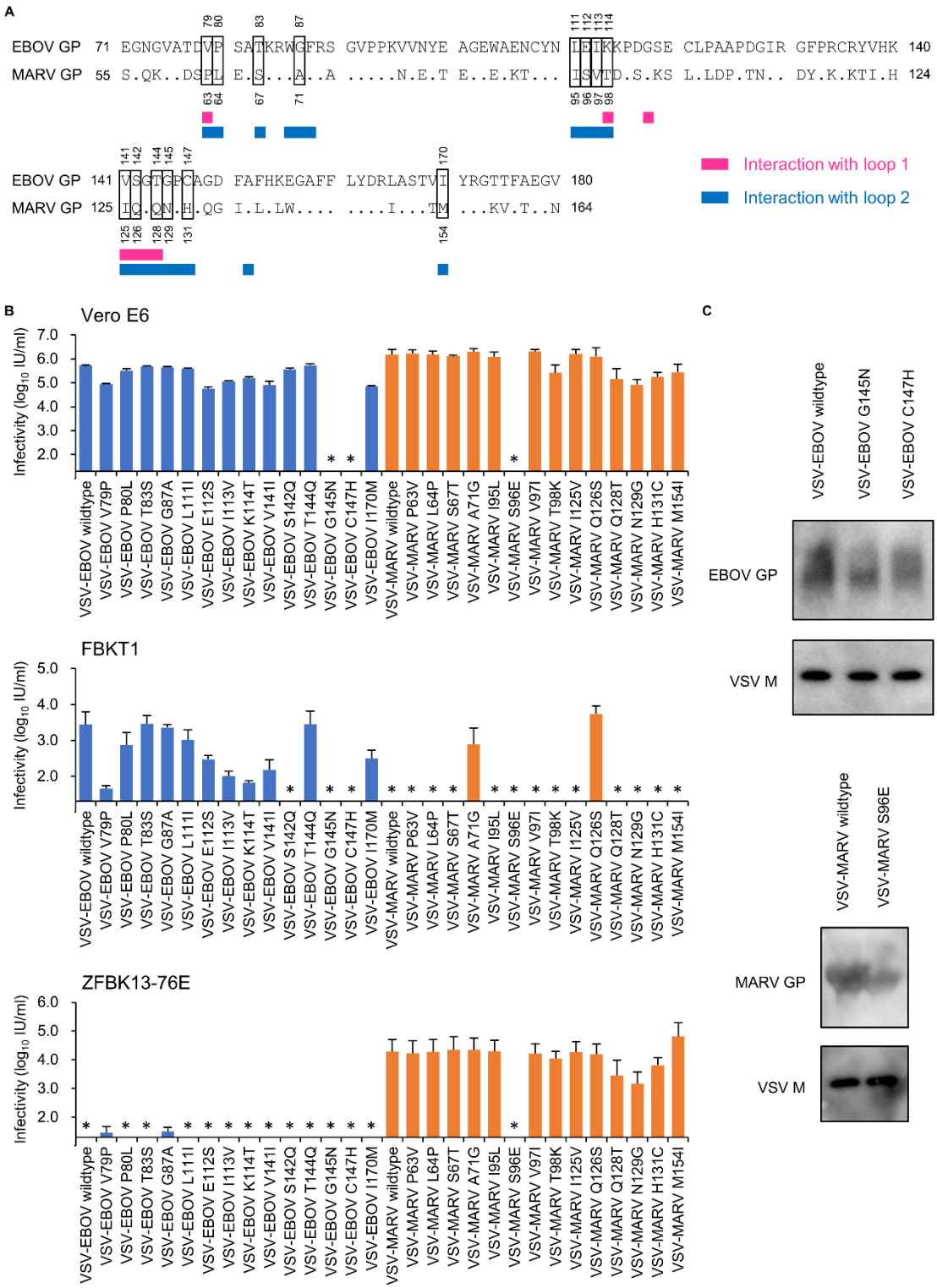
A
EBOV GP 71 EGNGVATDVP SATKRWGFRS GVPPKVVNYE AGEWAENCYN IEIKKPDGSE CLPAAPDGIR GFPRCRYVHK 140
MARV GP 55 S.QK..DSPL E.QG...A..A .....N.E.T E..E.KT... TSVTD.S.KS L.LDP.TN.. DY.K.KTI.H 124
EBOV GP 141 VSGTGPCAGD FAFHKEGAFF LYDRLASTVI YRGTTFAEGV 180
MARV GP 125 TQ.QN.H.QG I.L.LW.... ....I...TM ...KV.T..N 164
Interaction with loop 1
Interaction with loop 2
B
Vero E6
FBKT1
ZFBK13-76E
Infectivity (log10 IU/ml)
VSV-EBOV wildtype
VSV-EBOV V79P
VSV-EBOV P80L
VSV-EBOV T83S
VSV-EBOV G87A
VSV-EBOV L111I
VSV-EBOV E112S
VSV-EBOV I113V
VSV-EBOV K114T
VSV-EBOV V141I
VSV-EBOV S142Q
VSV-EBOV T144Q
VSV-EBOV G145N
VSV-EBOV C147H
VSV-EBOV I170M
VSV-MARV wildtype
VSV-MARV P63V
VSV-MARV L64P
VSV-MARV S67T
VSV-MARV A71G
VSV-MARV I95L
VSV-MARV S96E
VSV-MARV V97I
VSV-MARV T98K
VSV-MARV I125V
VSV-MARV Q126S
VSV-MARV Q128T
VSV-MARV N129G
VSV-MARV H131C
VSV-MARV M154I
C
VSV-EBOV wildtype
VSV-EBOV G145N
VSV-EBOV C147H
EBOV GP
VSV M
VSV-MARV wildtype
VSV-MARV S96E
MARV GP
VSV M

Figure 7. Infectivities of VSVs pseudotyped with wildtype and mutant GPs in FBKT1 and ZFBK13-76E cells

(A) Deduced amino acid sequences of the RBD of EBOV and MARV GPs are aligned. The amino acid residues at positions 79, 80, 83, 87, 111, 112, 113, 114, 141, 142, 144, 145, 147, and 170 (EBOV numbering), which were predicted to interact with the amino acid residues in loop1 and 2 of human NPC1-C and different between EBOV and MARV GP, are enclosed by rectangles. (B) Vero E6, FBKT1, and ZFBK13-76E cells were infected with VSVs pseudotyped with wildtype and mutant GPs of EBOV and MARV. Viral IUs in each cell line were determined by counting the number of GFP-expressing cells. Each experiment was conducted three times, and averages and standard deviations are shown. Asterisks represent IUs under the limit of detection (20 IU/ml). VSV-EBOV G145N, C147H, and VSV-MARV S96E could not be rescued likely due to the loss of GP function. (C) Western blotting for VSV-EBOV G145N, C147H, and VSV-MARV S96E to confirm GP expression and incorporation into VSV particles. Each virus was subjected to sodium dodecyl sulfate (SDS)-polyacrylamide gel electrophoresis followed by western blotting with mouse anti-EBOV GP monoclonal antibody (ZGP42/3.7), anti-MARV GP monoclonal antibody (AGP127-8), anti-VSV matrix protein antibody (VSV-M 195-2), horseradish peroxidase-conjugated goat anti-mouse IgG (115-035-062, Jackson ImmunoResearch). The bound antibodies were visualized with Immobilon Western (Millipore).

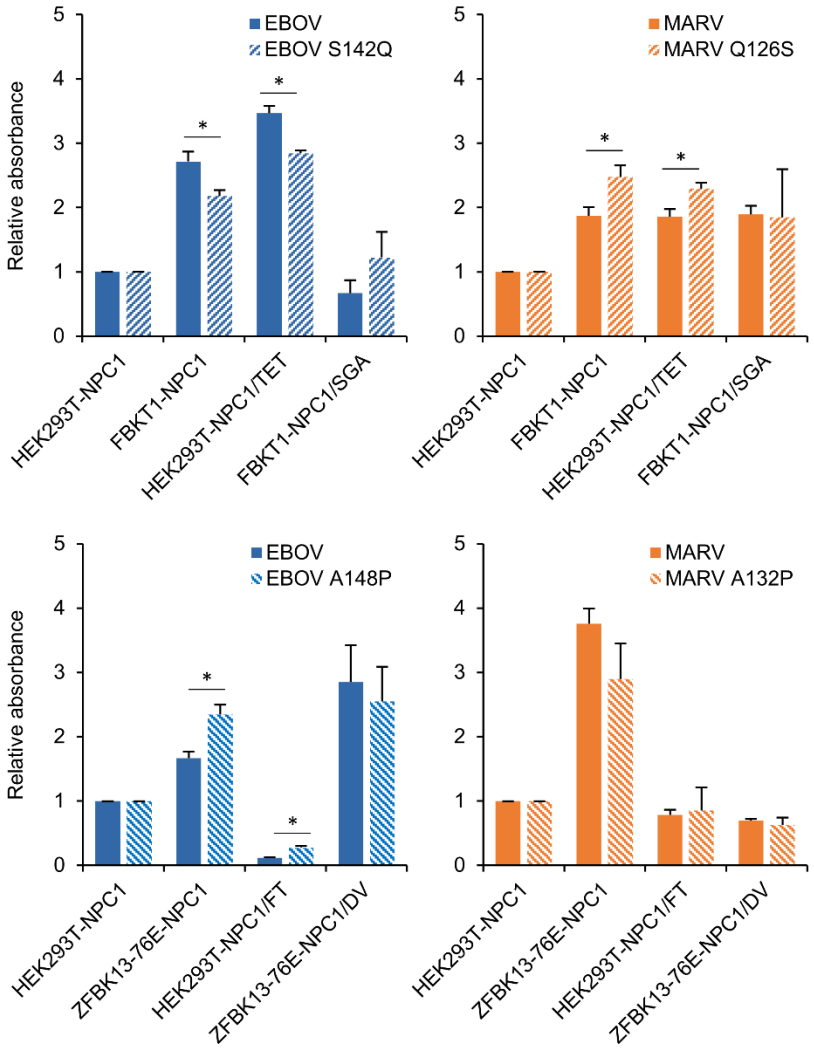

Figure 8. Binding activity of NPC1 molecules to wildtype and mutant GPs

A solid phase immunosorbent assay to detect binding activity of NPC1 and GP was carried out as described in the Materials and Method section. Each experiment was conducted three times and averages and standard deviations of relative OD values are shown. Significant differences are shown with asterisks (* $P < 0.05$).

Discussion

Bats are suspected to be the natural reservoirs of filoviruses. Although differences in their susceptibilities to each filovirus species have been suggested previously[12,31,45,60,66], the molecular mechanisms for these differences are poorly understood. In this study, I focused on the differential susceptibility of two bat-derived cell lines (FBKT1 and ZFBK13-76E) to MARV and EBOV infection. Site-directed mutagenesis revealed that three and two amino acid differences in the NPC1-C loop 1 and loop 2 regions, respectively, were essential for the preferred susceptibility of these bat cells either to EBOV or MARV infection (Figure 2), indicating that amino acid residues in both loop 1 and 2 regions are critical determinants for the host-range restriction of filoviruses.

The loop 1 region of FBKT1 NPC1 has the unique amino acid residues T, E, and T (TET) at positions 425, 426, and 427, whereas the corresponding amino acid residues of the other bat and primate cell lines tested in this study are S, G, and A (SGA, AGS, or SGS) (Figure 4B). I demonstrated that wildtype FBKT1 and transduced cell lines expressing NPC1 mutants with the TET residues were susceptible to EBOV GP-mediated, but not to MARV GP-mediated, infection (Figure 2 and Figure 5). Since the co-crystal structure of human NPC1-C and EBOV GP revealed that G426 of NPC1 was in direct contact with S142 of GP[86], it is conceivable that both TET and SGA residues of the loop 1 region interact with S142 of EBOV GP but that the TET residues are unable to interact with the corresponding residue (Q126) of MARV GP. I further confirmed this phenomenon using NPC1 mutants with single mutations at positions 426 (G or E) and found that these single mutations also switched the phonotypes of the NPC1-expresisng Vero E6 cells although the effect on the susceptibility was comparatively lower than 3

point mutations (i.e., SGA/TET) (Figure 10). Indeed, *in silico* structural analysis using the NPC1 and EBOV GP suggests that steric hindrance caused by the side chains of E426 of NPC1 and Q142 of GP likely impairs the interaction between these amino acid, which may explain reduced susceptibility of FBKT1 cells to MARV (Figure 9A). On the other hand, SUDV and RESTV GPs, as well as MARV GP, have Q at this position but VSV-SUDV and -RESTV infected FBKT1 cells to an extent similar to VSV-EBOV (Figure 2). Moreover, the amino acid substitution of Q142S did not significantly affect the infectivity of VSV-SUDV and -RESTV in FBKT1 cells (Figure 6D). Likewise, the amino acid substitution of S142Q had little effect on the infectivity of VSV-TAFV and -BDBV in FBKT1 cells (Figure 6D). These observations might suggest that the amino acid residue at position 142 (EBOV numbering) is less important for SUDV, RESTV, TAFV, and BDBV to infect FBKT1 cells than for EBOV and MARV. Interestingly, there is an amino acid difference between SUDV/RESTV/TAFV/BDBV and EBOV/MARV GPs (i.e., P in SUDV, RESTV, TAFV, and BDBV GPs, and A in EBOV and MARV GPs at position 148 [EBOV numbering]) (Figure 6C). The co-crystal structure of human NPC1-C and EBOV GP indicates that the position 148 is located adjacent to the GP RBD but at a distance from loop 1 of NPC1-C[86]. Although the amino acid residue at position 148 may not directly interact with loop 1, the amino acid difference at position 148 (A or P) might cause distortion of the conformation of the RBD, resulting in a change of the size and/or shape of the RBD cavity. A similar mechanism has been previously reported the substitution of amino acid residue V141A, which may not directly make contact with NPC1 loop 2, restored the NPC1 loop 2-dependent interaction with GP[70]. This mechanism might also explain the effect of the A71G substitution on the VSV-MARV infectivity in FBKT1 cells (Figure 7).

ZFBK13-76E NPC1 has unique amino acid residues F and T (FT) at positions 502 and 505 in the loop 2 region and the corresponding amino acid residues of the other cell lines were D and V (DV). I found that swapping of these amino acid between HEK293T and ZFBK13-76E NPC1 changed the susceptibility to EBOV and MARV infection (i.e., cells expressing NPC1 with the DV residues were susceptible to both EBOV and MARV and those with the FT residues were less susceptible to EBOV) (Figure 5). This suggests that the DV, but not FT, residues in NPC1 interact with EBOV GP efficiently. The *in silico* analysis indicates that V505 of NPC1 interacts with only T144 of EBOV GP through a hydrogen bond between backbone atoms, suggesting that the difference of the side chain between V and T might not affect the interaction with EBOV GP (data not shown). In contrast, a single amino acid substitution at residue 502 was shown to affect the susceptibility of *E. helvum* bat-derived cell lines to EBOV[60], suggesting that the amino acid difference at position 502 of NPC1 is a major determinant for the reduced susceptibility of ZFBK13-76E cells to EBOV infection. Since the hydrophobic character of amino acid residues at this position is substantially different between F and D, this amino acid difference might change the structure of loop 2, affecting the cell's susceptibility to EBOV infection. Indeed, point mutation at this position changed the susceptibility of the NPC1-expresisng Vero E6 cells although its effect was lower than 2 point mutations (i.e., DV/FT) (Figure 10). I demonstrated that the amino acid substitution of A148P of EBOV GP affected the infectivity of the pseudotyped VSV on ZFBK13-76E cells. The co-crystal structure of human NPC1-C and EBOV GP suggests that A148 directly makes contact with loop 2, and is located adjacent to the RBD (Figure 9B)[86]. *In silico* mutagenesis suggested that an A148P mutation of GP altered the size and/or shape of the hydrophobic cavity of the GP RBD (Figure 9B), which might

restore the interaction between GP and NPC1 having the D502F substitution.

The previous study showed that Niemann-Pick C2 (NPC2), a partner of NPC1 in low density lipoprotein-derived cholesterol transportation, binds to NPC1 using an interaction interface that is similar to that used by GP[42], raising the possibility that the competition between GP and NPC1 might be involved in the filovirus host tropism. In this study, I found that amino acid positions 425, 426, 427, 502, and 505 of NPC1 were important for the interaction with filovirus GP. It was suggested that amino acid positions 425-427 of NPC1 did not seem to be important for the interaction with NPC2 and that amino acid position 505 was not involved in the interaction with NPC2. Although it was also suggested that amino acid position 502 of NPC1 is important for the interaction with NPC2 (amino acid position 25; Lysine), I confirmed that this Lysine in NPC2 is conserved among human 293T, FBKT1, and ZFBK13-76E cells (data not shown). Thus, it is unlikely that NPC2 plays a major role in controlling the filovirus host tropism.

The Yaeyama flying fox, the origin of FBKT1 cells, is one of the subspecies of Ryukyu flying foxes (*Pteropus dasymallus*) distributed in Asian countries such as Japan, the Philippines, and Taiwan[85]. In the Philippines, RESTV infection was confirmed in bats, monkeys, and pigs[4,29,51,52]. Although filovirus infection of this bat species has never been reported, anti-RESTV antibodies were detected in a large flying fox (*Pteropus vampyrus* [*P. vampyrus*]), which is evolutionary related the to the Yaeyama flying fox[5,29]. Interestingly, the unique amino acid motif of loop 1 (i.e., TET found in FBKT1) has also been found in NPC1 of other fruit bat species, including the large flying fox (*P. vampyrus*) and the black flying fox (*Pteropus alecto*)[43], both of which are widely distributed in Asian and Oceanian countries (i.e., *P. vampyrus* in Brunei Darussalam, China, Indonesia, Malaysia, Myanmar, the Philippines, Singapore, Thailand, Timor-Leste, and Vietnam,

and *P. alecto* in Indonesia and Papua New Guinea)[6,74]. Considering the accumulating seroepidemiological evidence suggesting filovirus infection of wild animals in Asian countries such as China, Singapore, Bangladesh, and Indonesia[26,40,61,67,87,88,89], these fruit bat species may play a role in the ecology of ebolaviruses, including yet unknown species, while these data suggest the inability of MARV or MARV-related filoviruses (i.e., filoviruses that have Q at position 142 of GP [EBOV numbering]) to efficiently infect these bat species.

ZFBK13-76E cells are derived from the straw-colored fruit bat (*E. helvum*), which is widely distributed in sub-Saharan African countries[48]. It has been shown that this bat species migrates between the tropical forests of African countries[73]. Previous studies provided serological evidence of the infection of *E. helvum* bats with EBOV[25,64]. However, findings here, as well as the data published previously[60], suggest that this bat species may not be highly susceptible to EBOV. Serological cross-reactivity with multiple ebolavirus species or the existence of natural EBOV variants that have P at position 148 of GP may explain this contradictory observation. Alternatively, it is possible to assume that there might be polymorphism of the NPC1 gene in this same bat species and some minor populations of this species might be susceptible to EBOV. In addition, in these bats another factor besides NPC1 could play a role for filovirus infection. This remains to be clarified in future studies.

In this study, I have demonstrated that GP-NPC1 engagement is one of the genetic determinants of the host-range restriction of filoviruses in bat species. Interestingly, *R. aegyptiacus* bats were not fully susceptible to ebolaviruses when infected experimentally[31], whereas cell lines derived from this bat species (e.g., ZFBK15-137RA) were susceptible to VSVs pseudotyped with GPs of ebolaviruses (Figure 2) and infectious

ebolaviruses[28,36,39,50,60]. Thus, some other host factors (e.g., those involved in the immune system) that interact with viral proteins may play an additional role in determining the susceptibility of bats to filoviruses. Indeed, unique functions of bat interferon (IFN) and IFN-induced proteins, as well as IFN-inhibitory viral proteins, have been reported previously[19,47,68,76,90]. Further biological and bioinformatic analyses with a larger number of bats and bat-derived cell lines and their genomic sequences are required to better understand the molecular basis of virus-host protein interactions involved in the filovirus host tropism.

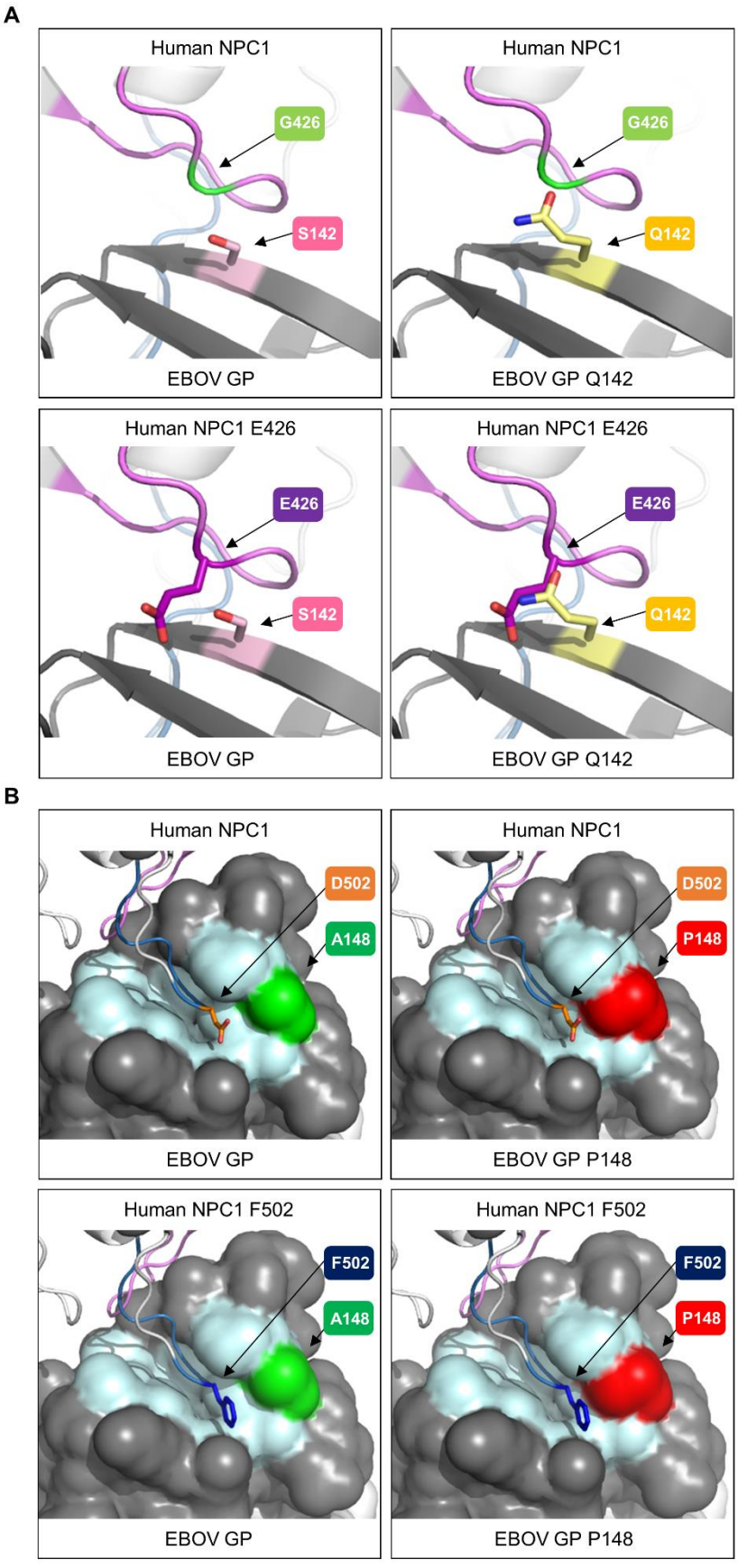
A
Human NPC1
G426
S142
EBOV GP
Human NPC1
G426
Q142
EBOV GP Q142
Human NPC1 E426
E426
S142
EBOV GP
Human NPC1 E426
E426
Q142
EBOV GP Q142
B
Human NPC1
D502
A148
EBOV GP
Human NPC1
D502
P148
EBOV GP P148
Human NPC1 F502
F502
A148
EBOV GP
Human NPC1 F502
F502
P148
EBOV GP P148

Figure 9. Predicted structure of the NPC1 loops and EBOV GP

(A, B) The three-dimensional co-crystal structure of domain C of human NPC1 and EBOV GP (PDB ID: 5F1B) was used as a template. The amino acid residues G426 or D502 of NPC1 and S142 or A148 of EBOV GP were substituted to E426 or F502 and Q142 or P148 by *in silico* mutagenesis. (A) The interface of NPC1 loop 1 and EBOV GP is shown as a ribbon model. G426/E426 of NPC1 and S142/Q142 of GP are shown in light green/purple and pink/yellow, respectively. (B) Loop 2 of NPC1 is shown as a ribbon model. GP1 (dark grey) and GP2 (light grey) are shown in a surface model. The amino acid residues forming a hydrophobic cavity of GP1 (i.e., V79, P80, T83, W86, G87, F88, L111, E112, I113, V141, G145, P146, C147, A152, and I170) are colored light cyan. D502/F502 of NPC1 and A148/P148 of GP are shown in orange/dark blue and green/deep red, respectively. Nitrogen and oxygen atoms in side chains are shown in blue and red, respectively (A, B). All mutagenesis procedures were performed using PyMOL (Schrödinger LLC).

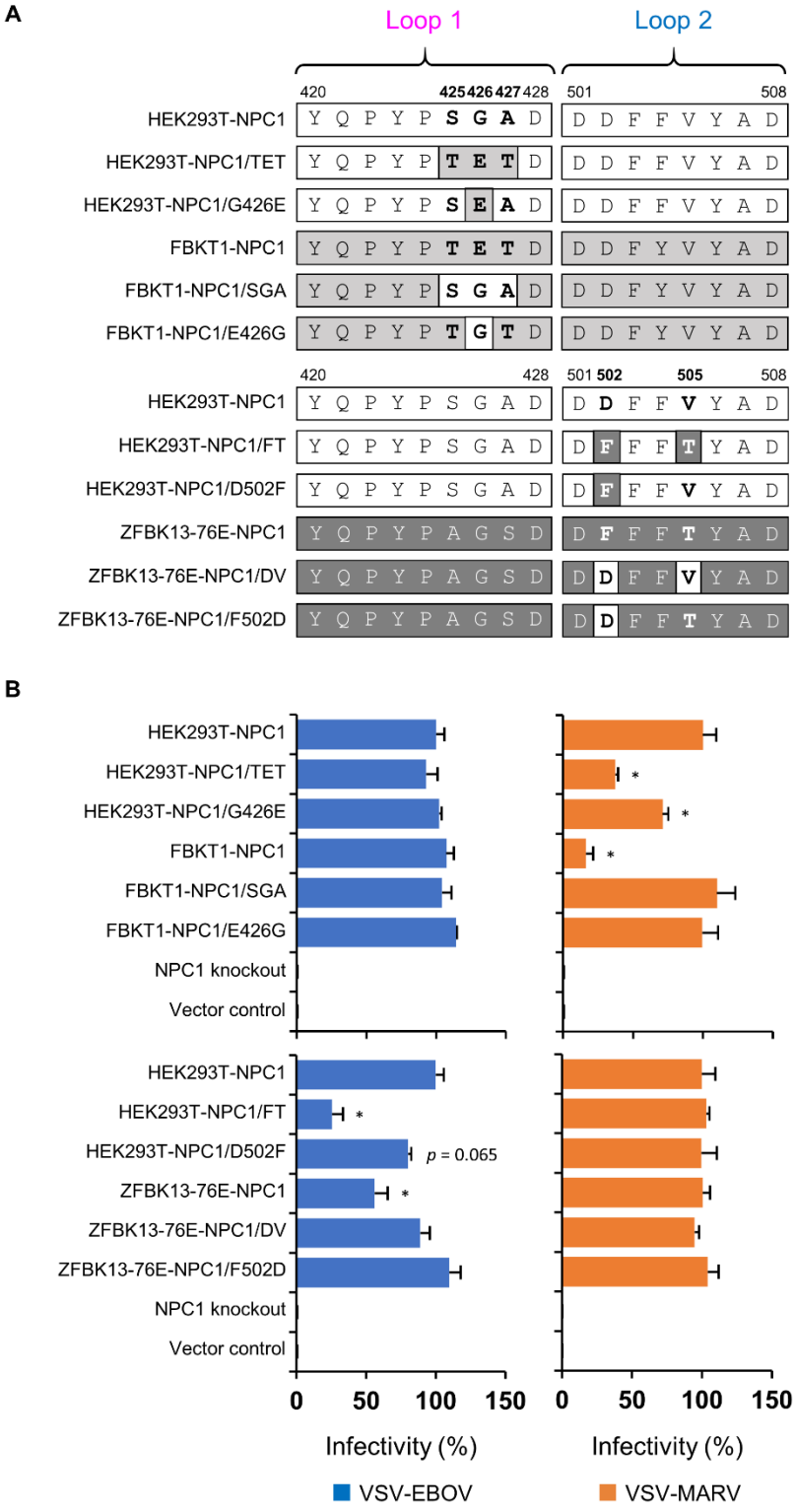
A
Loop 1
Loop 2
420
425 426 427 428
501
508
HEK293T-NPC1
HEK293T-NPC1/TET
HEK293T-NPC1/G426E
FBKT1-NPC1
FBKT1-NPC1/SGA
FBKT1-NPC1/E426G
420
428
501 502
505
508
HEK293T-NPC1
HEK293T-NPC1/FT
HEK293T-NPC1/D502F
ZFBK13-76E-NPC1
ZFBK13-76E-NPC1/DV
ZFBK13-76E-NPC1/F502D
B
HEK293T-NPC1
HEK293T-NPC1/TET
HEK293T-NPC1/G426E
FBKT1-NPC1
FBKT1-NPC1/SGA
FBKT1-NPC1/E426G
NPC1 knockout
Vector control
HEK293T-NPC1
HEK293T-NPC1/FT
HEK293T-NPC1/D502F
p = 0.065
ZFBK13-76E-NPC1
ZFBK13-76E-NPC1/DV
ZFBK13-76E-NPC1/F502D
NPC1 knockout
Vector control
0
50
100
150
Infectivity (%)
VSV-EBOV
0
50
100
150
Infectivity (%)
VSV-MARV

Figure 10. Effects of amino acid substitutions in the NPC1-C loops on cell susceptibility to pseudotyped VSVs

(A) Wildtype and mutant NPC1 genes were constructed to assess the importance of the unique amino acid sequences (shown in boldface) in loop 1 of FBKT1 and loop 2 of ZFBK13-76E. (B) Vero E6/NPC1-KO cl.19 cells transduced with exogenous NPC1 genes and control cells (NPC1 knockout and Vector control) were infected with pseudotyped VSVs. Relative infectivity was determined as described in Materials and Methods. Each experiment was conducted three times, and averages and standard deviations are shown. For comparison of viral infectivity among NPC1-expressing cells, one-way analysis of variance was performed, followed by Dunnett's test, and significant differences compared to cells expressing wildtype human NPC1 (HEK293T-NPC1) are shown (* $P < 0.05$).

Summary

Fruit bats are suspected to be natural hosts of filoviruses, including EBOV and MARV. Interestingly, however, previous studies have suggested that these viruses have different tropisms depending on the bat species. Here, I show a molecular basis underlying the host-range restriction of filoviruses. I found that bat-derived cell lines FBKT1 (*Pteropus dasymallus yayeyamae*) and ZFBK13-76E (*E. helvum*) showed preferential susceptibility to EBOV and MARV, respectively, whereas the other bat cell lines tested were similarly infected with both viruses. In FBKT1 and ZFBK13-76E, unique amino acid sequences (i.e., TET at positions 425-427 and F/T at positions 502/505 in FBKT1 and ZFBK13-76E, respectively) were found in the domain C loops of NPC1 protein, one of the cellular receptors interacting with the filovirus GP. I generated Vero E6 cells expressing wildtype and mutant NPC1 proteins and found that these cell lines show differential susceptibility to EBOV and MARV. Substitutions of amino acid residues in the NPC1-interacting site among filovirus GPs altered the infectivity of pseudotyped VSVs in two bat cell lines. Taken together, these findings indicate that the heterogeneity of bat NPC1 orthologues is an essential factor controlling filovirus species-specific host tropism.

Chapter II:

Niemann-Pick C1-mediated distinctive host cell preference for a bat-derived filovirus, Lloviu virus

Introduction

In 2002, a novel filovirus, LLOV, phylogenetically distinct from the viruses in the genera *Ebolavirus* and *Marburgvirus*, was discovered in carcasses of insectivorous bats (Schreiber's bent-winged bat: *Miniopterus schreibersii*) in Spain[57]. Based on the phylogenetic data, and this virus has been designated as a new filovirus member belonging to the genus *Cuevavirus*[2,20]. In 2016, LLOV was detected again in the same species of bats in Hungary[34]. More recently, the full-length genomes of previously unknown filoviruses (i.e., BOMV and MLAV) were also discovered in bats[23,57,87]. Taken together, the frequent detection of filoviruses in bats suggests that this animal species is closely related to the ecology of filoviruses.

Since infectious LLOV particles have never been isolated, the biological properties of LLOV remain unclear. Previous studies suggest that LLOV GP is the only glycoprotein responsible for viral entry into cells[45,80]. Like other filoviruses, LLOV GP is thought to play a major role in the replication of filoviruses and has been shown to have the potential to mediate viral entry into mammalian cells, including cells from both human and bat origins[45,59]. It has also been shown that viral protein (VP) 24 and VP35, which are known to suppress the innate immune response and play an important role in the pathogenicity of EBOV and/or MARV[47], are also encoded in the LLOV genome. Both LLOV VP24 and VP35 were shown to antagonize immune responses in human cells[19]. These findings suggest that LLOV has the capacity to infect a wide variety of mammalian

cells and may be a potential pathogen for humans.

In general, the host range and specificity of viruses (i.e., cell susceptibility) are determined by multiple viral and host factors. One of the most important steps in this lifecycle is entry of the viruses into the host cells, which is generally mediated by interaction between viral surface proteins and host cell receptors[79]. Previous studies suggest that each filovirus might have a preference for an individual bat species[28,60], which is principally determined by the interaction between GPs and filovirus receptors. Maruyama *et al* previously compared the susceptibility of different bat-derived cell lines to filoviruses using VSV pseudotyped with GPs[45] and found that a cell line (i.e., SuBK12-08)-derived from a bat (*Miniopterus* sp.) showed a preferential susceptibility to LLOV[45]. However, the molecular mechanisms underlying this preferential cell susceptibility remain unknown. In this study, I focused on the interaction between GP and a host cellular receptor, NPC1 protein[9,15], and found that heterogeneity of NPC1-C, which interacts with filovirus GP[37,86], is important for the distinctive cell tropism of LLOV to the particular bat cell line.

Materials and Methods

Cells

Vero E6 cells were grown in DMEM (Sigma) supplemented with 10% fetal calf serum (Cell Culture Bioscience), 100 U/ml penicillin, and 0.1 mg/ml streptomycin (Gibco). Bat-derived cell lines were established as described previously[77]. All of the bat cell lines were grown in RPMI 1640 medium (Sigma) supplemented with 10% FCS, 100 U/ml penicillin, and 0.1 mg/ml streptomycin. Origins of these cell lines are shown in Table 1. Origin of SuBK12-08 cells were identified by morphology, habitat, and BLAST searches using the sequences from the cytochrome *b* gene[49]. Vero E6/NPC1-KO cl.19, and Vero E6/NPC1-KO cl.19 expressing exogenous NPC1 derived from HEK293T, FBKT1, and ZFBK13-76E cells, were established previously[35,81].

Viruses

Using VSV containing the green fluorescent protein gene instead of the receptor binding VSV G protein gene, pseudotyped viruses with GPs of EBOV (Mayinga), MARV (Angola), and LLOV (Asturias) (VSV-EBOV, -MARV, and -LLOV) were generated as described previously[45,80]. The mutant GP genes were constructed by site-directed mutagenesis. VSVs pseudotyped with filovirus GPs were pre-incubated with an anti-VSV G monoclonal antibody, VSV-G [N] 1-9[54], to abolish any background infection with parental VSV. Pseudotyped VSVs were inoculated into confluent cell monolayers cultured on 96-well plates, and IUs in each cell line were determined for each cell line twenty hours later by counting the number of GFP-expressing cells under a fluorescent microscope. Relative infectivity of pseudotyped VSVs in bat-derived cell lines was determined by setting the GFP-positive cell number of Vero E6 cells infected with each

virus to 100%. Relative infectivity of pseudotyped VSVs in a NPC1-knockout Vero E6 cell line (Vero E6/NPC1-KO cl.19) expressing exogenous NPC1 were determined by setting the GFP-positive cell number of wildtype HEK293T NPC1-expressing cells infected with each virus to 100%.

Cloning of bat NPC1 genes and generation of stable cell lines expressing chimeric HEK293T/SuBK12-08 NPC1 proteins

I used the nucleotide sequences of NPC1 genes derived from FBKT1, ZFBK13-76E, ZFBK11-97, ZFBK15-137RA, DemKT1 SuBK12-08, YubFKT1, and BKT1, which have been determined previously (GenBank accession numbers; LC462999, LC462993, LC462994, LC462995, LC462996, LC462997, LC462271, and LC462998, respectively[81]). The NPC1 gene of SuBK12-08 was amplified with KOD One (TOYOBO) and inserted into a pSP72 (Promega) plasmid vector. After sequence confirmation, domain C of the NPC1 gene fragment derived from SuBK12-08 cells (amino acid residues 377-624 [373-620 in HEK293T NPC1 numbering]) and the NPC1 gene fragment derived from HEK293T cells (amino acid residues 1-372 and 621-1279) were amplified with KOD One. Then, these NPC1 gene fragments were inserted into the pMXs-puro retroviral vector (Cell Biolabs) to construct pMXs-chimeric HEK293T/SuBK12-08 NPC1. An In-Fusion cloning kit (BD Clontech) was used to construct the retroviral vectors carrying these NPC1 genes. Using pMXs-chimeric HEK293T/SuBK12-08 NPC1, Vero E6 cells expressing chimeric HEK293T/SuBK12-08 NPC1 was generated as described previously[81]. Briefly, retroviruses carrying NPC1 genes were generated using Platinum GP cells (Cell Biolabs). Vero E6/NPC1-KO cl.19 cells[81] were infected with these retroviruses and the NPC1-transduced cells were selected with puromycin (Sigma

Aldrich). I examined the expression levels of exogenous NPC1 molecules by western blotting using anti-NPC1 monoclonal antibody (ab6276. Abcam) and horseradish peroxidase-conjugated goat anti-mouse IgG (115-035-062. Jackson ImmunoResearch). I confirmed that similar band intensities were uniformly observed in each cell line (data not shown).

Statistical analysis

All statistical analyses were performed using R software (version 3.5.2)[71]. For comparison of viral infectivity between NPC1-transduced cell lines and infectivity of pseudotyped VSVs among wildtype and mutant viruses in SuBK12-08 cells, one-way analysis of variance, followed by the Dunnett's test were performed (Figure 12 and 13). For the comparison of viral infectivity of pseudotyped VSVs between VSV-EBOV/V141A and -EBOV/V141A&S142K and VSV-LLOV/A150V and -LLOV/A150V&K151S in SuBK12-08 cells (Figure 13), Student *t*-test was used. *P*-values of less than 0.05 were considered to be significant.

Results

Susceptibility of bat-derived cell lines to VSV-EBOV, -MARV, and -LLOV

Using replication-incompetent VSVs pseudotyped with GPs of EBOV, MARV, and LLOV, I investigated GP-dependent tropism, which is hypothesized to be the primary determinant for cell susceptibilities to filoviruses. Vero E6 cells, which are generally used for filovirus studies and eight bat-derived cell lines from different origins (i.e., five frugivorous bat species in the suborder Megachiroptera [FBKT1, ZFBK13-76E, ZFBK11-97, ZFBK15-137RA, and DemKT1] and three insectivorous bat species in the suborder Microchiroptera [SuBK12-08, YubFKT1, and BKT1]) were used to compare their susceptibilities (Table 1, Figure 11). I found that SuBK12-08, a cell line derived from the *Miniopterus* sp., showed higher susceptibility to VSV-LLOV than VSV-EBOV and -MARV, although cell lines derived from the other bat species including two insectivorous bat species did not show such preferential susceptibility to VSV-LLOV. Interestingly, VSV-MARV infected most of the bat-derived cells at relatively high infectivity, except FBKT1 and ZFBK13-76E cells.

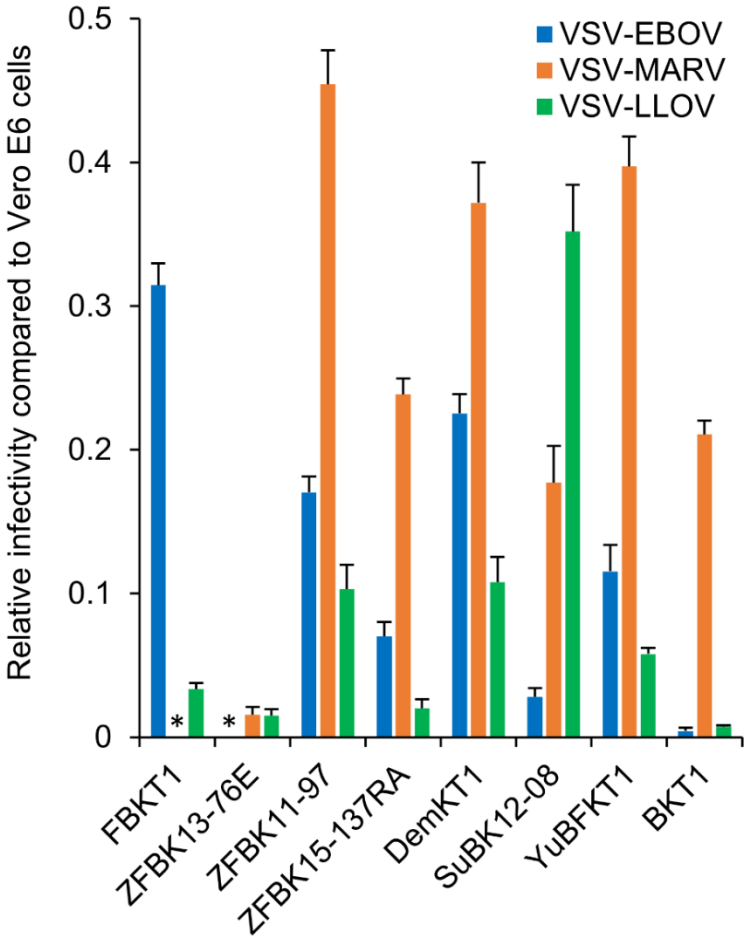

Figure 11. Susceptibility of bat-derived cell lines to VSVs pseudotyped with filovirus GPs

Vero E6 and bat-derived cells were infected with VSVs pseudotyped with filovirus GPs (VSV-EBOV, -MARV, and -LLOV). Relative infectivity of pseudotyped VSVs in bat-derived cell lines was determined as described in Materials and Methods. Each experiment was conducted three times, and average and standard deviations are shown. Asterisks represent IUs under the limit of detection (20 IU/ml).

Amino acid sequences of the domain C of bat NPC1 orthologues and susceptibilities of Vero E6 cell lines expressing exogenous NPC1 proteins to VSV-EBOV, -MARV, and -LLOV

Since pseudotyped VSVs rely on GP-dependent entry into cells, I assumed that the interaction between GP and its receptor is important for the preferential susceptibility of SuBK12-08 cells to VSV-LLOV. Indeed, the interaction between GP and NPC1, which is believed to be the receptor for all known filoviruses, including LLOV and newly identified filoviruses[23,58,87], has been demonstrated to control the host specificity of filoviruses[35,56,60,81]. Thus, I compared amino acid sequences of bat NPC1-C region which include two loop structures that have been shown to directly interact with the RBD of GP[37,86] (Figure 12A). Although there were no unique sequences in the NPC1-C loop regions of SuBK12-08 cells and amino acid residues in the loops of its NPC1-C region were conserved among three insectivorous bat species, SuBK12-08, YuBFKT1, and BKT1, I found a unique amino acid residue (i.e., lysine) at position 416 in SuBK12-08, near the NPC1-C loop 1, whereas the other two insectivorous bat cell lines had asparagine or aspartic acid.

To ascertain whether the difference in the NPC1 sequence between SuBK12-08 and other bat cell lines affected the cell susceptibility to pseudotyped VSVs, I generated Vero E6 cells stably expressing exogenous NPC1 proteins derived from SuBK12-08, HEK293T, FBKT1, and ZFBK13-76E, which were generated and used in the previous study[81] and compared their susceptibilities to pseudotyped VSVs (Figure 12B). Since the full-length sequence of the open reading frame of SuBK12-08 NPC1 was not available, I constructed chimeric NPC1 that had the SuBK12-08-drived domain C in HEK293T NPC1 (See Materials and Methods). I found that infectivity of VSV-EBOV in cells

expressing chimeric HEK293T/SuBK12-08 NPC1 was slightly but significantly lower than those in the cells expressing NPC1 of HEK293T. The infectivity of VSV-MARV in chimeric HEK293T/SuBK12-08 NPC1-expressing cells was similar to that in HEK293T NPC1 cells. In contrast, the infectivity of VSV-LLOV in the cells expressing chimeric HEK293T/SuBK12-08 NPC1 was significantly higher than that in the HEK293T NPC1-expressing cells. Interestingly, cells expressing FBKT1 NPC1 showed reduced susceptibility to VSV-LLOV. In addition, VSV-EBOV and VSV-MARV less efficiently infected the cells expressing ZFBK13-76E and FBKT1 NPC1, respectively, which was consistent with the previous findings[81].

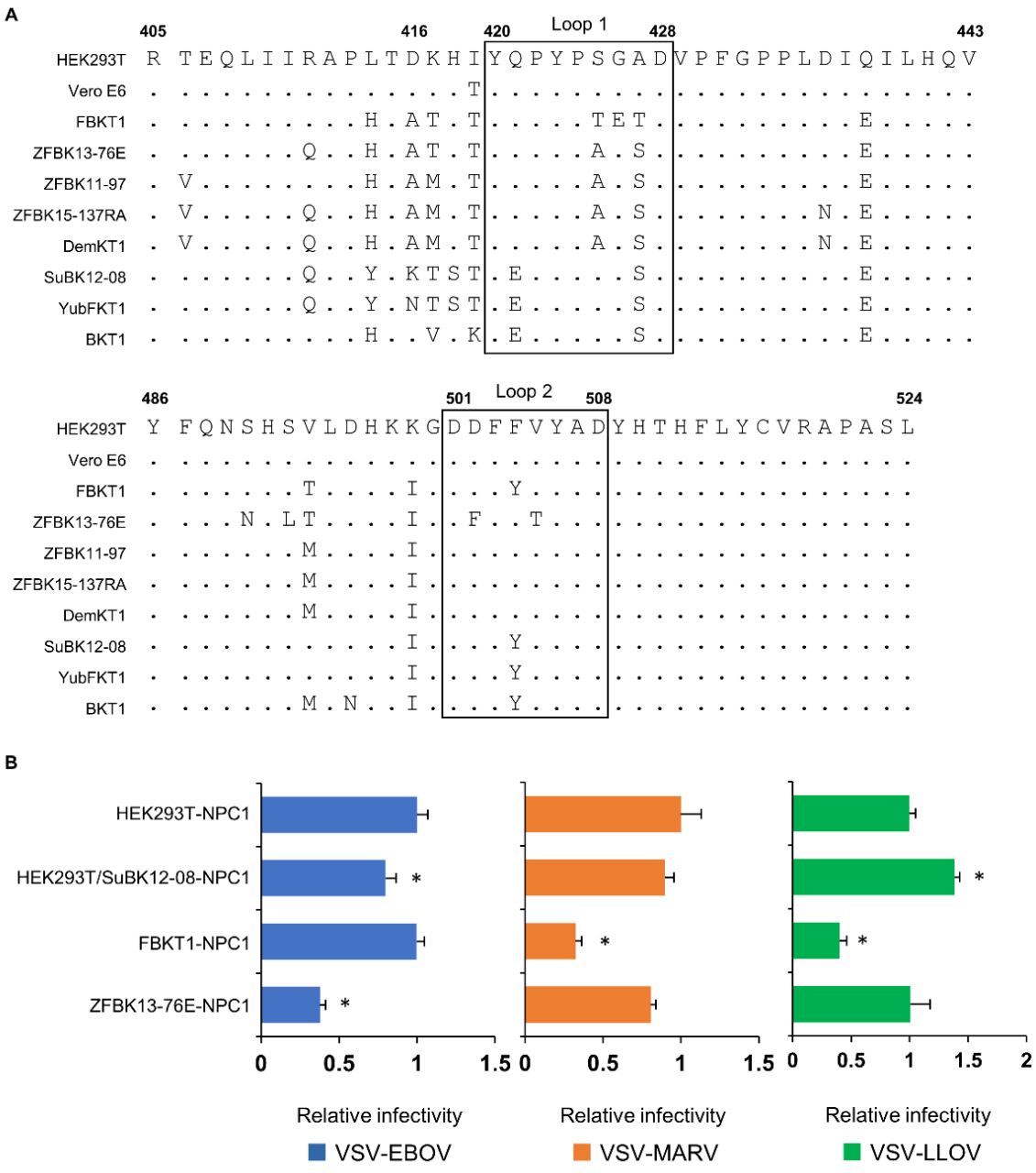

Figure 12. Comparison of amino acid sequences of the domain C of bat NPC1 orthologues and susceptibility of NPC1-transduced cell lines to pseudotyped VSVs

(A) Deduced amino acid sequences of the NPC1-C sequences of FBKT1, ZFBK13-76E, ZFBK11-97, ZFBK15-137RA, DemKT1, SuBK12-08, YubFKT1, and BKT1, are aligned. Amino acid positions of loop 1 and loop 2 are enclosed by rectangles. (B) Vero E6/NPC1-KO cl.19 cells transduced with exogenous NPC1 genes were infected with pseudotyped VSVs. Relative infectivity was determined as described in Materials and

Methods. Each experiment was conducted three time, and averages and standard deviations are shown. For comparison of viral infectivity among NPC1-expresisng cells, one-way analysis of variance followed by the Dunnett's test were performed, and significant differences compared to the cells expressing wildtype human NPC1 (HEK293T-NPC1) are shown (* $P < 0.05$).

Comparison of amino acid sequences at the NPC1-binding interface of filovirus GP and the infectivity of VSV pseudotyped with EBOV, LLOV, and their mutant GPs in SuBK12-08 cells

The previously determined co-crystal structure of human NPC1-C and EBOV GP demonstrated that the GP RBD contains key amino acid residues that directly interact with some of the amino acid residues in the loop structures of NPC1-C[86]. Thus, I compared amino acid sequences around this region between EBOV and LLOV GPs (Figure 13A) and found five amino acid differences at positions 79, 114, 141, 142, and 144 (EBOV numbering); valine (V), lysine (K), V, serine (S), and threonine (T) in EBOV GP and leucine (L), T, alanine (A), K, and A in LLOV GP at the corresponding amino acid positions.

To determine the important amino acid residues for the differential infectivity of VSV-LLOV and -EBOV in SuBK12-08 cells, I generated VSVs pseudotyped with GP mutants whose amino acid at position 79, 114, 141, 142, or 144 (EBOV numbering) was swapped between LLOV and EBOV GPs and their infectivity were compared using Vero E6 and SuBK12-08 cells (Figure 13B). Though there were no significant differences among the VSV-EBOV, -EBOV V79L, -EBOV K114T, -EBOV S142K, and -EBOV T144A in the infectivity in SuBK12-08 cells, VSV-EBOV V141A was shown to infect SuBK12-08 cells more efficiently. On the other hand, while I found little difference in the infectivity among VSV-LLOV, -LLOV L88V, -LLOV T123K, and -LLOV A153T in SuBK12-08 cells, the infectivity of VSV-LLOV A150V and -LLOV K151S were significantly lower than that of VSV-LLOV. I also determined the importance of double amino acid substitutions (i.e., V141A and S142K in EBOV GP and A150V and K151S in LLOV GP) for the infectivity of VSV-LLOV and -EBOV in this *Miniopterus* bat cell line.

While there was no significant difference between VSV-EBOV V141A and -EBOV V141A&S142K in the infectivity of SuBK12-08 cells, the double amino acid substitution (i.e., A150V and K151S) in LLOV GP decreased the infectivity of VSV-LLOV more efficiently than either of the single amino acid substitutions. These results indicate that the amino acid residue V at position 141 in EBOV GP and A/K at positions 150/151 in LLOV GP play a major role in the different potential of EBOV and LLOV GP to mediate virus entry into SuBK12-08 cells.

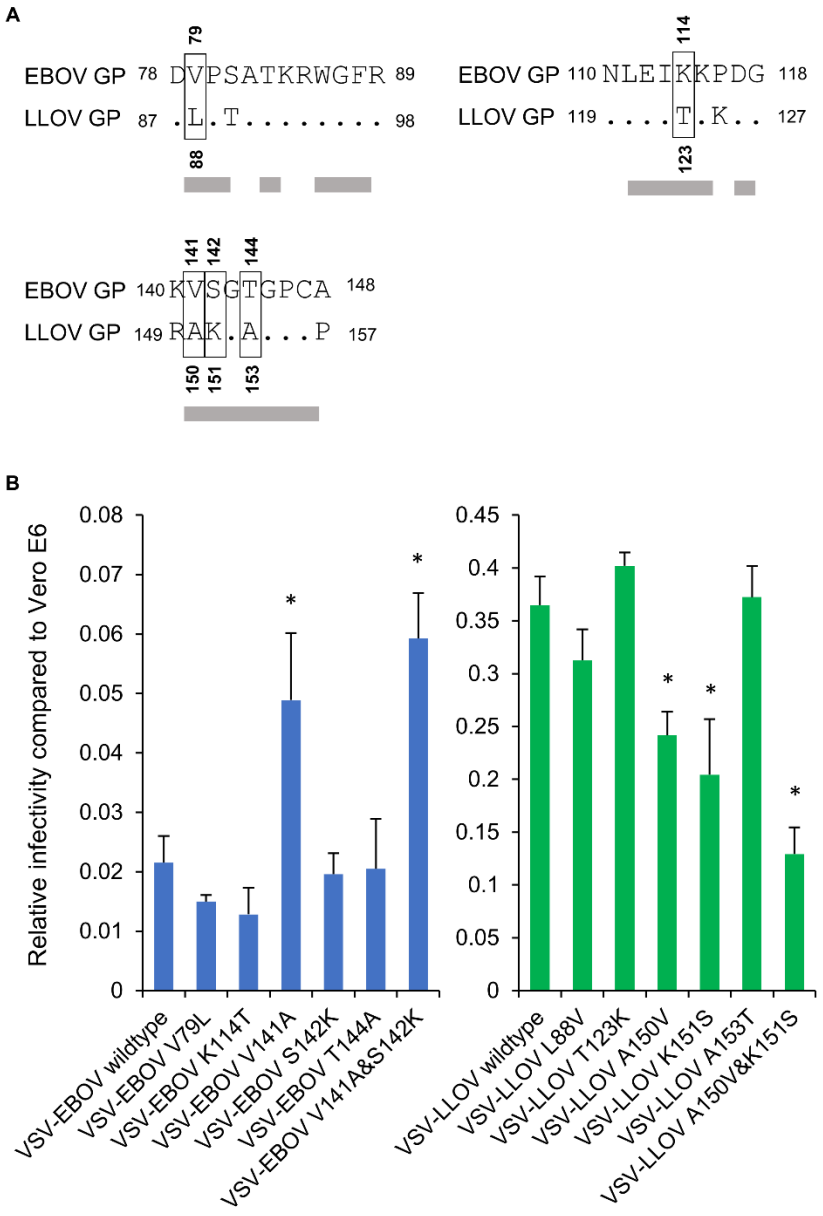

Figure 13. Amino acid differences in the RBD between EBOV and LLOV GPs and effects of amino acid substitutions in the GP RBD on the infectivity of pseudotyped VSVs in SuBK12-08 cells

(A) Deduced amino acid sequences of EBOV and LLOV GPs are aligned. The amino acid residues at positions 79, 114, 141, 142, and, 144 (EBOV numbering) which are assumed to interact with the amino acid in loop 1 and loop 2 of human NPC1-C, are enclosed by rectangles. (B) Vero E6 and SuBK12-08 cells were infected with VSVs pseudotyped with EBOV, LLOV and their mutant GPs. Relative infectivity was determined as described in Materials and Methods. Each experiment was conducted three times, and averages and standard deviations are shown.

Discussion

Although the biological properties of LLOV remain poorly studied[8,19,33,34,45,60,72], it has been shown that the LLOV GP has potential to mediate viral entry into many mammalian cell lines. Previously, I compared the susceptibility of bat-derived cell lines to filoviruses, using VSVs pseudotyped with filovirus GPs, and found that VSV pseudotyped with LLOV GP showed relatively higher infectivity to a cell line derived from a *Miniopterus* bat (*Miniopterus* sp.) than the other bat cell lines tested (Figure 11)[45], indicating that LLOV has preferential tropism to this bat species. In this study, I investigated the molecular mechanisms underlying the cell preference of LLOV.

NPC1 is a ubiquitous receptor for filoviruses including LLOV[9,15,58] and has been shown to be required for the cellular entry of filoviruses and is thus important for their host range restriction and host specificity[35,56,60,81]. In this study, I focused on the interaction between GP and NPC1 to explain cell tropism of LLOV. I found that the NPC1 protein of SuBK12-08 cells had the potential to mediate LLOV infection more efficiently than those of the other bat origins tested (Figure 12B). Although I found no unique amino acid residues in the two GP-interacting loop regions of SuBK12-08 NPC1-C, there is a distinctive amino acid residue (i.e., K at position 416) adjacent to the loop 1 region (Figure 12A). I hypothesize that this amino acid difference affects the loop 1 structure, resulting in the increased interaction between NPC1 and LLOV GP.

I found two amino acid differences between LLOV and EBOV GPs (i.e., V and A at position 141, S and K at position 142: EBOV numbering) were responsible for the different cell preference of pseudotyped VSVs in SuBK12-08 cells (Figure 13B). It has been shown that V141 and S142 of EBOV GP interact with amino acid residues in the loop 1 of NPC1-C, more strongly than those in the loop 2 of NPC1-C[86]. Therefore, these

results support my hypothesis that the mechanism for the preferential tropism of LLOV in *Miniopterus* bats may be a result of strengthened interactions between GP and loop 1 of the NPC1-C.

Schreiber's bent-winged bat (*M.schreibersii*) is an insectivorous bat distributed in southern Palearctic, Ethiopic, Oriental, and Australian regions[7]. Since the discovery of LLOV in Spain[57], anti-LLOV antibodies have been detected in *M. schreibersii* bats in Spain in 2015 and the LLOV RNA genome has been detected in a *M. schreibersii* bat in Hungary in 2016[34,72]. These studies suggest that this bat species may be a preferred host for LLOV. Accordingly, there was a significant difference in the seroprevalence of LLOV infection between bat species (i.e., 36.5% in *M. schreibersii* bats and 0% in *Eptesicus serotine* bats), suggesting that this bat species (*M. schreibersii*) is highly susceptible to LLOV[72] and may become a source of spread for LLOV to other potential animal species including humans and other bats. On the other hand, it still remains unknown whether this bat species is the natural host of LLOV since LLOV seems to be pathogenic in this bat species[34,57].

In this study, I demonstrated that the interaction between GP and NPC1 is one of the factors controlling the preferential susceptibility of *Miniopterus* bat cells to LLOV. Recently, the genomes of new filoviruses were discovered from some bat species; BOMV from little free-tailed bats (*Chaerephon pumilus*) and Angolan free-tailed bats (*Mops condylurus*) and MLAV from Rousettus bats (*Rousettus* sp.)[23,87]. The host range of these new viruses will be of interest to the filovirus community as both BOMV and MLAV GPs were shown to utilize NPC1 as a host cell receptor[23,87]. To understand the whole picture of filovirus ecology, it is important to determine the host specificity of newly identified filoviruses as well as previously known human-pathogenic ebolaviruses and

marburgviruses.

Summary

LLOV, a bat-derived filovirus phylogenetically distinct from human-pathogenic filoviruses such as EBOV and MARV, has been discovered in Europe. However, since infectious LLOV particles have not been isolated, the biological properties of this virus remain poorly understood. Previously, I found that VSV-LLOV showed higher infectivity in an insectivorous bat (*Miniopterus* sp.)-derived cell line than to the other bat-derived cell line tested, which was distinct from the tropism of VSV-EBOV and VSV-MARV. In this study, I investigated the mechanisms underlying this preference by focusing on the interaction between GP and the NPC1 protein, one of the known cellular receptors of filoviruses. Cloned NPC1 genes from human and some bat species including *Miniopterus* sp. were introduced to NPC1-knockout Vero E6 cells and their susceptibility to VSV-LLOV and -EBOV were compared. I found that the cell line expressing *Miniopterus* bat-derived NPC1 showed higher susceptibility to VSV-LLOV than the cells expressing NPC1 derived from human or the other bat cell lines tested. Swapping of some amino acid residues in the NPC1-binding site between LLOV and EBOV GPs exchanged the infectivity of VSV-LLOV and VSV-EBOV in the *Miniopterus* bat-derived cell line. These results suggest that the interaction between GP and NPC1 is important for the tropism of LLOV to *Miniopterus* bats.

Conclusion

Although bats are suspected to be the natural reservoir of filoviruses, previous studies have suggested that the viruses have different tropisms depending on the species of bat that acts as a host. However, the mechanisms that determine this tropism and host range are poorly understood. In this thesis, I investigated the molecular determinants for distinctive susceptibilities of bat-derived cell lines (i.e., FBKT1, ZFBK13-76E, and SuBK12-08 cells) to filoviruses, focusing on the interaction between GP and NPC1 protein, which is required for filovirus entry into cells.

In chapter I, I determined the molecular mechanism for the impaired susceptibility of FBKT1 and ZFBK13-76E cells to MARV and EBOV, respectively. The unique amino acid sequences in the NPC1-C loop regions (i.e., TET at positions 425-427 and F/T at positions 502/505 in FBKT1 and ZFBK13-76E, respectively) were found to be important for the differential susceptibility of the two bat cell lines to MARV and EBOV. Amino acid residues important for the interaction of the NPC1 loops and these bat cell lines were also identified within the receptor binding sites of EBOV and MARV GPs. *In silico* structural analysis and site-directed mutagenesis suggest that E426 and F502 of NPC1 play critical roles in reducing the susceptibility of FBKT1 and ZFBK13-76E cells to MARV and EBOV, respectively.

In chapter II, I investigated the molecular mechanism involved in the preferential susceptibility of SuBK12-08 cells to LLOV, which was discovered in *Miniopterus schreibersii* bats from Europe. I found that NPC1 derived from SuBK12-08 cells had increased potential to mediate VSV-LLOV entry, compared to those derived from human or the other bat cell lines tested. Site-directed mutagenesis indicated that amino acid residues at positions A150 and K151 of the NPC1-interacting site of LLOV GPs were

important for this preferential tropism. Since SuBK12-08 has a unique amino acid residue adjacent to the loop 1 region of NPC1-C (i.e., K at position 416), this amino acid residue is likely to be important in the higher susceptibility of SuBK12-08 cells to LLOV.

In this thesis, I determined a molecular basis underlying the host-range restriction of filoviruses. This study provides fundamental information which allows us to better understand of the filovirus ecology. This is a prerequisite in minimizing the risk of filovirus transmission from wildlife to humans. Identification of natural reservoirs and potential intermediate hosts for these viruses is required to prevent and control filovirus infection in future.

Acknowledgments

I express my deepest gratitude to my supervisor, Prof. Ayato Takada (Division of Global Epidemiology, Research Center for Zoonosis Control [CZC], Hokkaido University [HU]), whose comments and suggestions were invaluable throughout the course of this PhD. I thank him for his support of my overseas activities and conference attendance, which forced me to grow and gave me confidence. I thank him for being my mentor and teacher over the past several years.

I sincerely appreciate the invaluable support and advice provided by Prof. Hideaki Higashi (Division of Infection and Immunity, CZC, HU), Prof. Hirofumi Sawa (Division of Molecular Pathobiology, CZC, HU), and Prof. Yoshihiro Sakoda (Laboratory of Microbiology, Graduate School of Veterinary Medicine, HU), during the experimental portion of my thesis. Each of you has given advice that has helped me to refine my PhD and expand my research skills.

I am deeply grateful to Associate Prof. Manabu Igarashi, Specially Appointed Assistant Prof. Reiko Yoshida, Specially Appointed Assistant Prof. Rashid Manzoor, and Specially Appointed Assistant Prof. Masahiro Kajihara (Division of Global Epidemiology, CZC, HU) for their technical and intellectual support.

I would like to thank Dr. Heinz Feldmann, Dr. Andrea Marzi, Ms. Kay Menk, Dr. Atsushi Okumura, Dr. Wakako Furuyama, (National Institute of Allergy and Infectious Diseases, National Institutes of Health, Rocky Mountain Laboratories), Dr. Yoshimi Tsuda (Department of Microbiology, Graduate School of Medicine, HU), and all the employees at Rocky Mountain Laboratories for their technical supports, thoughtful advice and cooperation.

I am also deeply grateful to Assistant Prof. Hirohito Ogawa (Graduate School of

Medicine, Dentistry and Pharmaceutical Sciences, Okayama University), Assistant Prof. Yongjin Qiu, Dr. Hayato Harima (Hokudai Center for Zoonosis Control in Zambia, School of Veterinary Medicine, University of Zambia), Mr. Yoshiki Eto (Division of Global Epidemiology, CZC, HU) for their support during my stay in Zambia.

I would like to thank Associate Prof. Alexander N. Freiberg, Dr. Terence E. Hill, Dr. Junki Maruyama (Department of Pathology, University of Texas Medical Branch), Prof, Ken Maeda (National Institutes of Infectious Diseases), and Prof. Eiichi Hondo (Laboratory of Animal Morphology, Graduate School of Bioagricultural Sciences, Nagoya University) for their technical support and their provision of important materials (e.g., bat-derived cell lines).

I am grateful to the coordinator at the Program for Leading Graduate Schools, HU, Prof. Motohiro Horiuchi (Laboratory of Veterinary Hygiene, Graduate School of Veterinary Medicine, HU), and the members of the Leading Program Office for their help with my PhD coursework.

I thank, Dr. Naganori Nao, Dr. Tatsunari Kondoh, Dr. Masahiro Sato, Ms. Hiroko Miyamoto, Ms. Asako Shigeno and Ms. Akina Mori-Kajihara (Division of Global Epidemiology, CZC, HU) for their advice and suggestions. I also thank Mr. Kosuke Okuya, Mr. Takeshi Saito, Mr. Mao Isono, Mr. Boniface Lombe Pongombo, Ms. Yurie Kida, Ms. Nodoka Kasajima, and Mr. Takanari Hattori (Division of Global Epidemiology, CZC, HU) for their daily assistance. I wish to thank all the member of CZC for their help, encouragement, and kindness.

I also express my deep gratitude to my family for their understanding and financial supports for a long period.

Finally, my research was funded by the Research Fellowship for Young

Scientists from the Japan Society for the Promotion of Science.

Abstract in Japanese

フィロウイルス科は進化系統学的に５属（*Ebolavirus* 属、*Marburgvirus* 属、*Cuevavirus* 属、*Striavirus* 属、*Thamnovirus* 属）に分類され、計９種類のウイルス（*Ebolavirus* 属; Ebola virus [EBOV]、Sudan virus、Taï Forest virus、Bundibugyo virus、Reston virus、*Marburgvirus* 属; Marburg virus [MARV]、*Cuevavirus* 属; Lloviu virus [LLOV]、*Striavirus* 属; Xīlǎng virus、*Thamnovirus* 属; Huángjiāo virus）が見つかっている。EBOV および MARV を代表とする、*Ebolavirus* 属および *Marburgvirus* 属に含まれるウイルスはヒトを含む霊長類動物に重篤な出血熱を引き起こす事が知られている。フィロウイルス感染症のヒトでの報告は中央および西アフリカ内に限定しているが、アジアやヨーロッパ諸国に生息する動物におけるフィロウイルスの感染例も報告されている。

コウモリはフィロウイルスの自然宿主として有力視されているが、コウモリ種間でのフィロウイルスに対する感受性が大きく異なることが示唆されている。しかし、感受性の違いを決定する因子は殆ど不明である。本学位論文ではフィロウイルスのレセプターの一つである Niemann-Pick C1 (NPC1)とウイルス粒子表面糖蛋白質(GP)との相互作用に着目し、コウモリのフィロウイルスに対する感受性を決定する分子機構を解析した。

第一章では、ヒトを含む霊長類動物に高い病原性を示す EBOV および MARV に対するコウモリの感受性を決定する分子機構を解析した。まず、異なる 8 種のコウモリに由来する細胞を用いて、EBOV および MARV の GP を持つシュードタイプ水疱性口炎ウイルスならびに感染性の EBOV および MARV に対する感受性を比較した結果、ヤエヤマオオコウモリ由来の細胞株 FBKT1 およびストローオオコウモリ由来の細胞株 ZFBK13-76E が、それぞれ MARV および EBOV に対して殆ど感受性を示さない事が分かった。そこで、GP のレセプター結合部位

が相互作用する NPC1 分子上のドメイン C 領域（フィロウイルスのレセプターとしての機能に重要なドメイン）に存在する loop 領域のアミノ酸配列（420 番目から 428 番目[loop1 領域]、および 501 番目から 508 番目のアミノ酸残基 [loop2 領域]）を、8 種のコウモリ間で比較したところ、FBKT1 および ZFBK13-76E の loop 領域には、他のコウモリにはみられない特徴的な配列が認められた（FBKT1 では loop1 領域内に T425、E426、T427、ZFBK13-76E では loop2 領域内に F502、T505）。次に、EBOV および MARV の両方に対して高い感受性を示すヒト由来の細胞株 HEK293T の NPC1 の loop 領域にそれらの特徴的な配列を導入した NPC1 変異体を作出し、NPC1 をノックアウトした Vero E6 細胞に発現させ、EBOV および MARV に対する感受性を比較した。その結果、FBKT1 と ZFBK13-76E の配列を導入した NPC1 変異体を発現する細胞では、それぞれ MARV および EBOV に対する感受性の低下が見られた。また、FBKT1 および ZFBK13-76E の NPC1 の loop 領域に HEK293T 由来の配列を導入した NPC1 変異体を発現させた細胞では、MARV および EBOV に対する感受性に差が認められなかった。さらに、loop 領域と相互作用する GP のレセプター結合領域に MARV と EBOV 間で異なるアミノ酸が存在することから、それらを入れ替えたウイルスを作出し、FBKT1 および ZFBK13-76E における感染性を比較した結果、MARV の GP の Q126 あるいは EBOV の GP の A148 が FBKT1 あるいは ZFBK13-76E におけるウイルスの感染性に関与することが分った。さらに、*in silico* 構造解析ならびに 1 アミノ酸変異を持つ NPC1 発現細胞を用いた解析を実施した結果、NPC1 の loop 領域上に存在する E426 および F502 が、それぞれ MARV に対する FBKT1 の感受性および EBOV に対する ZFBK13-76E の感受性の決定において中心的な役割を果たしている事が示唆された。以上の結果により、コウモリ種間における NPC1 loop 領域のアミノ酸配列の僅かな違いが MARV および EBOV に対する感

受性を決定する重要な因子であることが示唆された。

2002 年、スペインの洞窟内に生息する食虫コウモリの死体から、*Ebolavirus* 属および *Marburgvirus* 属のウイルスとは進化系統学的に異なるフィロウイルスが発見され、LLOV と名づけられた。第 2 章では LLOV に対するコウモリの感受性を比較し、異なる感受性を決定する分子機構を解析した。まず、異なる 8 種のコウモリに由来する細胞を用いて、EBOV および LLOV の GP を持つシュードタイプウイルスに対する感受性を比較した。その結果、食虫コウモリである *Miniopterus* sp.由来の細胞株 SuBK12-08 細胞が LLOV に高い感受性を示すが、EBOV には殆ど感受性を示さない事が判明した。そこで、NPC1 分子の loop 領域のアミノ酸配列を、8 種のコウモリ間で比較したところ、SuBK12-08 の loop1 領域の近傍には、他のコウモリにはみられないアミノ酸残基 K416 が確認された。次に HEK293T 由来の NPC1 に SuBK12-08 由来の NPC1 のドメイン C 領域を導入したキメラ NPC1 を作出し、NPC1 をノックアウトした Vero E6 細胞に発現させ、EBOV および LLOV に対する感受性を比較した。その結果、SuBK12-08 由来の NPC1 ドメイン C を発現させた細胞は、ヒトおよび他種のコウモリ由来の NPC1 を発現させた細胞に比べて、LLOV に対する感受性の上昇および EBOV に対する感受性の低下が確認された。また、GP の NPC1 結合領域に EBOV および LLOV 間で複数の異なるアミノ酸配列が存在する事から、それらを交換したウイルスの SuBK12-08 への感染性を比較した結果、A150 および K151 が SuBK12-08 における LLOV の感染性に関与している事が判明した。以上の結果により、コウモリ種間における NPC1 のアミノ酸配列の違いが LLOV に対する細胞感受性を決定する因子である事が示唆された。

本研究により、フィロウイルスの宿主域を決定するメカニズムの一端が明らかとなった。フィロウイルスの生態の解明は、野生動物からヒトへのウイルス伝

播を未然に防ぐために重要である。今後、フィロウイルスによる感染症の予防と制圧のためには、その自然宿主とヒトへの伝播を仲介する感受性動物の特定が必要となる。

References

1) Alvarez CP, Lasala F, Carrillo J, Muñiz O, Corbí AL, Delgado R. C-type lectins DC-SIGN and L-SIGN mediate cellular entry by Ebola virus in cis and in trans. J Virol 76, 6841-6844, 2002.

2) Amarasinghe GK, Arechiga Ceballos NG, Banyard AC, Basler CF, Bavari S, Bennett AJ, Blasdell KR, Briese T, Bukreyev A, Cai Y, Calisher CH, Campos Lawson C, Chandran K, Chapman CA, Chiu CY, Choi KS, Collins PL, Dietzgen RG, Dolja VV, Dolnik O, Domier LL, Durrwald R, Dye JM, Easton AJ, Ebihara H, Echevarria JE, Fooks AR, Formenty PBH, Fouchier RAM, Freuling CM, Ghedin E, Goldberg TL, Hewson R, Horie M, Hyndman TH, Jiang D, Kityo R, Kobinger GP, Kondo H, Koonin EV, Krupovic M, Kurath G, Lamb RA, Lee B, Leroy EM, Maes P, Maisner A, Marston DA, Mor SK, Muller T, Muhlberger E, Ramirez VMN, Netesov SV, Ng TFF, Nowotny N, Palacios G, Patterson JL, Paweska JT, Payne SL, Prieto K, Rima BK, Rota P, Rubbenstroth D, Schwemmle M, Siddell S, Smither SJ, Song Q, Song T, Stenglein MD, Stone DM, Takada A, Tesh RB, Thomazelli LM, Tomonaga K, Tordo N, Towner JS, Vasilakis N, Vazquez-Moron S, Verdugo C, Volchkov VE, Wahl V, Walker PJ, Wang D, Wang LF, Wellehan JFX, Wiley MR, Whitfield AE, Wolf YI, Ye G, Zhang YZ, Kuhn JH. Taxonomy of the order Mononegavirales: update 2018. Arch Virol 163, 2283-2294, 2018.

3) Amman BR, Carroll SA, Reed ZD, Sealy TK, Balinandi S, Swanepoel R, Kemp A, Erickson BR, Comer JA, Campbell S, Cannon DL, Khristova ML, Atimnedi P, Paddock CD, Crockett RJ, Flietstra TD, Warfield KL, Unfer R, Katongole-Mbidde E, Downing R, Tappero JW, Zaki SR, Rollin PE, Ksiazek TG, Nichol ST, Towner JS. Seasonal pulses of Marburg virus circulation in juvenile *Rousettus aegyptiacus* bats coincide with periods of increased risk of human infection. PLoS Pathog 8, e1002877, 2012.

4) Barrette RW, Metwally SA, Rowland JM, Xu L, Zaki SR, Nichol ST, Rollin PE, Towner JS, Shieh WJ, Batten B, Sealy TK, Carrillo C, Moran KE, Bracht AJ, Mayr GA, Sirios-Cruz M, Catbagan DP, Lautner EA, Ksiazek TG, White WR, McIntosh MT. Discovery of swine as a host for the Reston ebolavirus. Science 325, 204-206, 2009.

5) Bastian ST, Jr., Tanaka K, Anunciado RV, Natural NG, Sumalde AC, Namikawa T. Evolutionary relationships of flying foxes (genus *Pteropus*) in the Philippines inferred from DNA sequences of cytochrome b gene. Biochem Genet 40, 101-116, 2002.

6) Bates P, Francis, C., Gumal, M., Bumrungsri, S., Walston, J., Heaney, L., and Mildenstein, T. *Pteropus vampyrus* The IUCN Red List of Threatened Species 2008, e.T18766A8593657., 2008.

7) Benda P, Paunović, M. . *Miniopterus schreibersii*. The IUCN Red List of Threatened Species 2019 e.T81633057A22103918. , 2019.

8) Brinkmann A, Ergunay K, Radonic A, Kocak Tufan Z, Domingo C, Nitsche A. Development and preliminary evaluation of a multiplexed amplification and next generation sequencing method for viral hemorrhagic fever diagnostics. PLoS Negl Trop Dis 11, e0006075, 2017.

9) Carette JE, Raaben M, Wong AC, Herbert AS, Obernosterer G, Mulherkar N, Kuehne AI, Kranzusch PJ, Griffin AM, Ruthel G, Dal Cin P, Dye JM, Whelan SP, Chandran K, Brummelkamp TR. Ebola virus entry requires the cholesterol transporter Niemann-Pick C1. Nature 477, 340-343, 2011.

10) Carstea ED, Morris JA, Coleman KG, Loftus SK, Zhang D, Cummings C, Gu J, Rosenfeld MA, Pavan WJ, Krizman DB, Nagle J, Polymeropoulos MH, Sturley SL, Ioannou YA, Higgins ME, Comly M, Cooney A, Brown A, Kaneski CR, Blanchette-Mackie EJ, Dwyer NK, Neufeld EB, Chang TY, Liscum L, Strauss JF, 3rd, Ohno K, Zeigler M, Carmi R, Sokol J, Markie D, O'Neill RR, van Diggelen OP, Elleder M, Patterson MC, Brady RO, Vanier MT, Pentchev PG, Tagle DA. Niemann-Pick C1 disease gene: homology to mediators of cholesterol homeostasis. Science 277, 228-231, 1997.

11) Chandran K, Sullivan NJ, Felbor U, Whelan SP, Cunningham JM. Endosomal proteolysis of the Ebola virus glycoprotein is necessary for infection. Science 308, 1643-1645, 2005.

12) Changula K, Kajihara M, Mori-Kajihara A, Eto Y, Miyamoto H, Yoshida R, Shigeno A, Hang'ombe B, Qiu Y, Mwizabi D, Squarre D, Ndebe J, Ogawa H, Harima H, Simulundu E, Moonga L, Kapila P, Furuyama W, Kondoh T, Sato M, Takadate Y, Kaneko C, Nakao R, Mukonka V, Mweene A, Takada A. Seroprevalence of filovirus infection of *Rousettus aegyptiacus* bats in Zambia. J Infect Dis 218, S312-S317, 2018.

13) Changula K, Kajihara M, Mweene AS, Takada A. Ebola and Marburg virus diseases in Africa: increased risk of outbreaks in previously unaffected areas? Microbiol Immunol 58, 483-491, 2014.

14) Changula K, Yoshida R, Noyori O, Marzi A, Miyamoto H, Ishijima M, Yokoyama A, Kajihara M, Feldmann H, Mweene AS, Takada A. Mapping of conserved and species-specific antibody epitopes on the Ebola virus nucleoprotein. Virus Res

176, 83-90, 2013.
15) Cote M, Misasi J, Ren T, Bruchez A, Lee K, Filone CM, Hensley L, Li Q, Ory D, Chandran K, Cunningham J. Small molecule inhibitors reveal Niemann-Pick C1 is essential for Ebola virus infection. Nature 477, 344-348, 2011.
16) Cruz JC, Sugii S, Yu C, Chang TY. Role of Niemann-Pick type C1 protein in intracellular trafficking of low density lipoprotein-derived cholesterol. J Biol Chem 275, 4013-4021, 2000.
17) Davies JP, Ioannou YA. Topological analysis of Niemann-Pick C1 protein reveals that the membrane orientation of the putative sterol-sensing domain is identical to those of 3-hydroxy-3-methylglutaryl-CoA reductase and sterol regulatory element binding protein cleavage-activating protein. J Biol Chem 275, 24367-24374, 2000.
18) Ebihara H, Theriault S, Neumann G, Alimonti JB, Geisbert JB, Hensley LE, Groseth A, Jones SM, Geisbert TW, Kawaoka Y, Feldmann H. In vitro and in vivo characterization of recombinant Ebola viruses expressing enhanced green fluorescent protein. J Infect Dis 196 Suppl 2, S313-322, 2007.
19) Feagins AR, Basler CF. Lloviu virus VP24 and VP35 proteins function as innate immune antagonists in human and bat cells. Virology 485, 145-152, 2015.
20) Feldmann H, Geisbert TW. Ebola haemorrhagic fever. Lancet 377, 849-862, 2011.
21) Furuyama W, Marzi A, Nanbo A, Haddock E, Maruyama J, Miyamoto H, Igarashi M, Yoshida R, Noyori O, Feldmann H, Takada A. Discovery of an antibody for pan-ebolavirus therapy. Sci Rep 6, 20514, 2016.
22) Glynn JR, Bower H, Johnson S, Houlihan CF, Montesano C, Scott JT, Semple MG, Bangura MS, Kamara AJ, Kamara O, Mansaray SH, Sesay D, Turay C, Dicks S, Wadoum REG, Colizzi V, Checchi F, Samuel D, Tedder RS. Asymptomatic infection and unrecognised Ebola virus disease in Ebola-affected households in Sierra Leone: a cross-sectional study using a new non-invasive assay for antibodies to Ebola virus. Lancet Infect Dis 17, 645-653, 2017.
23) Goldstein T, Anthony SJ, Gbakima A, Bird BH, Bangura J, Tremeau-Bravard A, Belaganahalli MN, Wells HL, Dhanota JK, Liang E, Grodus M, Jangra RK, DeJesus VA, Lasso G, Smith BR, Jambai A, Kamara BO, Kamara S, Bangura W, Monagin C, Shapira S, Johnson CK, Saylors K, Rubin EM, Chandran K, Lipkin WI, Mazet JAK. The discovery of Bombali virus adds further support for bats as hosts of ebolaviruses. Nat Microbiol 3, 1084-1089, 2018.
24) Gong X, Qian H, Zhou X, Wu J, Wan T, Cao P, Huang W, Zhao X, Wang X, Wang P, Shi Y, Gao GF, Zhou Q, Yan N. Structural insights into the Niemann-Pick C1 (NPC1)-mediated cholesterol transfer and Ebola infection. Cell 165, 1467-1478,

2016.

25) Hayman DT, Emmerich P, Yu M, Wang LF, Suu-Ire R, Fooks AR, Cunningham AA, Wood JL. Long-term survival of an urban fruit bat seropositive for Ebola and Lagos bat viruses. PLoS One 5, e11978, 2010.

26) He B, Feng Y, Zhang H, Xu L, Yang W, Zhang Y, Li X, Tu C. Filovirus RNA in Fruit Bats, China. Emerg Infect Dis 21, 1675-1677, 2015.

27) Higgins ME, Davies JP, Chen FW, Ioannou YA. Niemann-Pick C1 is a late endosome-resident protein that transiently associates with lysosomes and the trans-Golgi network. Mol Genet Metab 68, 1-13, 1999.

28) Hoffmann M, Gonzalez Hernandez M, Berger E, Marzi A, Pohlmann S. The glycoproteins of all filovirus species use the same host factors for entry into bat and human cells but entry efficiency is species dependent. PLoS One 11, e0149651, 2016.

29) Jayme SI, Field HE, de Jong C, Olival KJ, Marsh G, Tagtag AM, Hughes T, Bucad AC, Barr J, Azul RR, Retes LM, Foord A, Yu M, Cruz MS, Santos IJ, Lim TM, Benigno CC, Epstein JH, Wang LF, Daszak P, Newman SH. Molecular evidence of Ebola Reston virus infection in Philippine bats. Virol J 12, 107, 2015.

30) Jeffers SA, Sanders DA, Sanchez A. Covalent modifications of the ebola virus glycoprotein. J Virol 76, 12463-12472, 2002.

31) Jones ME, Schuh AJ, Amman BR, Sealy TK, Zaki SR, Nichol ST, Towner JS. Experimental inoculation of Egyptian Rousette bats (*Rousettus aegyptiacus*) with viruses of the Ebolavirus and Marburgvirus genera. Viruses 7, 3420-3442, 2015.

32) Kajihara M, Marzi A, Nakayama E, Noda T, Kuroda M, Manzoor R, Matsuno K, Feldmann H, Yoshida R, Kawaoka Y, Takada A. Inhibition of Marburg virus budding by nonneutralizing antibodies to the envelope glycoprotein. J Virol 86, 13467-13474, 2012.

33) Kamper L, Zierke L, Schmidt ML, Muller A, Wendt L, Brandt J, Hartmann E, Braun S, Holzerland J, Groseth A, Hoenen T. Assessment of the function and intergenus-compatibility of Ebola and Lloviu virus proteins. J Gen Virol 100, 760-772, 2019.

34) Kemenesi G, Kurucz K, Dallos B, Zana B, Foldes F, Boldogh S, Gorfol T, Carroll MW, Jakab F. Re-emergence of Lloviu virus in Miniopterus schreibersii bats, Hungary, 2016. Emerg Microbes Infect 7, 66, 2018.

35) Kondoh T, Letko M, Vincent J. Munster, Manzoor R, Maruyama J, Furuyama W, Miyamoto H, Shigeno A, Fujikura D, Takadate Y, Yoshida R, Igarashi M, Feldmann H, Marzi A, Takada A. Single nucleotide polymorphisms in human

NPC1 influence filovirus entry into cells. J Infect Dis 218, S397-S402, 2018.

36) Krahling V, Dolnik O, Kolesnikova L, Schmidt-Chanasit J, Jordan I, Sandig V, Gunther S, Becker S. Establishment of fruit bat cells (*Rousettus aegyptiacus*) as a model system for the investigation of filoviral infection. PLoS Negl Trop Dis 4, e802, 2010.

37) Krishnan A, Miller EH, Herbert AS, Ng M, Ndungo E, Whelan SP, Dye JM, Chandran K. Niemann-Pick C1 (NPC1)/NPC1-like1 chimeras define sequences critical for NPC1's function as a flovirus entry receptor. Viruses 4, 2471-2484, 2012.

38) Kuhl A, Hoffmann M, Muller MA, Munster VJ, Gnirss K, Kiene M, Tsegaye TS, Behrens G, Herrler G, Feldmann H, Drosten C, Pohlmann S. Comparative analysis of Ebola virus glycoprotein interactions with human and bat cells. J Infect Dis 204 Suppl 3, S840-849, 2011.

39) Kuzmin IV, Schwarz TM, Ilinykh PA, Jordan I, Ksiazek TG, Sachidanandam R, Basler CF, Bukreyev A. Innate immune responses of bat and human cells to filoviruses: Commonalities and distinctions. J Virol 91, 2017.

40) Laing ED, Mendenhall IH, Linster M, Low DHW, Chen Y, Yan L, Sterling SL, Borthwick S, Neves ES, Lim JSL, Skiles M, Lee BPY, Wang LF, Broder CC, Smith GJD. Serologic evidence of fruit bat exposure to filoviruses, Singapore, 2011-2016. Emerg Infect Dis 24, 114-117, 2018.

41) Leroy EM, Kumulungui B, Pourrut X, Rouquet P, Hassanin A, Yaba P, Delicat A, Paweska JT, Gonzalez JP, Swanepoel R. Fruit bats as reservoirs of Ebola virus. Nature 438, 575-576, 2005.

42) Li X, Saha P, Li J, Blobel G, Pfeffer SR. Clues to the mechanism of cholesterol transfer from the structure of NPC1 middle lumenal domain bound to NPC2. Proc Natl Acad Sci U S A 113, 10079-10084, 2016.

43) Lowe TM, Eddy SR. tRNAscan-SE: a program for improved detection of transfer RNA genes in genomic sequence. Nucleic Acids Res 25, 955-964, 1997.

44) Maeda K, Hondo E, Terakawa J, Kiso Y, Nakaichi N, Endoh D, Sakai K, Morikawa S, Mizutani T. Isolation of novel adenovirus from fruit bat (Pteropus dasymallus yayeyamae). Emerg Infect Dis 14, 347-349, 2008.

45) Maruyama J, Miyamoto H, Kajihara M, Ogawa H, Maeda K, Sakoda Y, Yoshida R, Takada A. Characterization of the envelope glycoprotein of a novel filovirus, Lloviu virus. J Virol 88, 99-109, 2014.

46) Maruyama J, Nao N, Miyamoto H, Maeda K, Ogawa H, Yoshida R, Igarashi M, Takada A. Characterization of the glycoproteins of bat-derived influenza viruses.

Virology 488, 43-50, 2016.

47) Messaoudi I, Amarasinghe GK, Basler CF. Filovirus pathogenesis and immune evasion: insights from Ebola virus and Marburg virus. Nat Rev Microbiol 13, 663-676, 2015.

48) Mickleburgh S, Hutson, A.M., Bergmans, W., Fahr, J., Racey, P.A. *Eidolon helvum*, The IUCN Red List of Threatened Species 2008, e.T7084A12824968., 2008.

49) Miller-Butterworth CM, Eick G, Jacobs DS, Schoeman MC, Harley EH. Genetic and phenotypic differences between South African long-fingered bats, with a global Miniopterine phylogeny. J Mammal 86, 1121-1135, 2005.

50) Miller MR, McMinn RJ, Misra V, Schountz T, Muller MA, Kurth A, Munster VJ. Broad and temperature independent replication potential of filoviruses on cells derived from old and new world bat species. J Infect Dis 214, S297-S302, 2016.

51) Miranda ME, Ksiazek TG, Retuya TJ, Khan AS, Sanchez A, Fulhorst CF, Rollin PE, Calaor AB, Manalo DL, Roces MC, Dayrit MM, Peters CJ. Epidemiology of Ebola (subtype Reston) virus in the Philippines, 1996. J Infect Dis 179 Suppl 1, S115-119, 1999.

52) Miranda ME, Miranda NL. Reston ebolavirus in humans and animals in the Philippines: a review. J Infect Dis 204 Suppl 3, S757-760, 2011.

53) Miranda ME, White ME, Dayrit MM, Hayes CG, Ksiazek TG, Burans JP. Seroepidemiological study of filovirus related to Ebola in the Philippines. Lancet 337, 425-426, 1991.

54) Nakayama E, Tomabechi D, Matsuno K, Kishida N, Yoshida R, Feldmann H, Takada A. Antibody-dependent enhancement of Marburg virus infection. J Infect Dis 204 Suppl 3, S978-985, 2011.

55) Nanbo A, Maruyama J, Imai M, Ujie M, Fujioka Y, Nishide S, Takada A, Ohba Y, Kawaoka Y. Ebola virus requires a host scramblase for externalization of phosphatidylserine on the surface of viral particles. PLoS Pathog 14, e1006848, 2018.

56) Ndungo E, Herbert AS, Raaben M, Obernosterer G, Biswas R, Miller EH, Wirchnianski AS, Carette JE, Brummelkamp TR, Whelan SP, Dye JM, Chandran K. A single residue in Ebola virus receptor NPC1 influences cellular host range in reptiles. mSphere 1, 2016.

57) Negredo A, Palacios G, Vazquez-Moron S, Gonzalez F, Dopazo H, Molero F, Juste J, Quetglas J, Savji N, de la Cruz Martinez M, Herrera JE, Pizarro M, Hutchison SK, Echevarria JE, Lipkin WI, Tenorio A. Discovery of an ebolavirus-like

filovirus in europe. PLoS Pathog 7, e1002304, 2011.

58) Ng M, Ndungo E, Jangra RK, Cai Y, Postnikova E, Radoshitzky SR, Dye JM, Ramirez de Arellano E, Negredo A, Palacios G, Kuhn JH, Chandran K. Cell entry by a novel European filovirus requires host endosomal cysteine proteases and Niemann-Pick C1. Virology 468-470, 637-646, 2014.

59) Ng M, Ndungo E, Jangra RK, Cai Y, Postnikova E, Radoshitzky SR, Dye JM, Ramirez de Arellano E, Negredo A, Palacios G, Kuhn JH, Chandran K. Cell entry by a novel European filovirus requires host endosomal cysteine proteases and Niemann-Pick C1. Virology 468-470, 637-646, 2014.

60) Ng M, Ndungo E, Kaczmarek ME, Herbert AS, Binger T, Kuehne AI, Jangra RK, Hawkins JA, Gifford RJ, Biswas R, Demogines A, James RM, Yu M, Brummelkamp TR, Drosten C, Wang LF, Kuhn JH, Muller MA, Dye JM, Sawyer SL, Chandran K. Filovirus receptor NPC1 contributes to species-specific patterns of ebolavirus susceptibility in bats. Elife 4, 2015.

61) Nidom CA, Nakayama E, Nidom RV, Alamudi MY, Daulay S, Dharmayanti IN, Dachlan YP, Amin M, Igarashi M, Miyamoto H, Yoshida R, Takada A. Serological evidence of Ebola virus infection in Indonesian orangutans. PLoS One 7, e40740, 2012.

62) Niwa H, Yamamura K, Miyazaki J. Efficient selection for high-expression transfectants with a novel eukaryotic vector. Gene 108, 193-199, 1991.

63) Ogawa H, Kajihara M, Nao N, Shigeno A, Fujikura D, Hang'ombe BM, Mweene AS, Mutemwa A, Squarre D, Yamada M, Higashi H, Sawa H, Takada A. Characterization of a novel bat adenovirus isolated from straw-colored fruit bat (*Eidolon helvum*). Viruses 9, 2017.

64) Ogawa H, Miyamoto H, Nakayama E, Yoshida R, Nakamura I, Sawa H, Ishii A, Thomas Y, Nakagawa E, Matsuno K, Kajihara M, Maruyama J, Nao N, Muramatsu M, Kuroda M, Simulundu E, Changula K, Hang'ombe B, Namangala B, Nambota A, Katampi J, Igarashi M, Ito K, Feldmann H, Sugimoto C, Moonga L, Mweene A, Takada A. Seroepidemiological prevalence of multiple species of filoviruses in fruit bats (*Eidolon helvum*) migrating in Africa. J Infect Dis 212 Suppl 2, S101-108, 2015.

65) Olival K, H. Epstein J, Wang L, Field H, Daszak P. Are bats unique viral reservoirs? New Directions in Conservation Medicine: Applied Cases of Ecological Health pp. 195-212, 2012.

66) Olival KJ, Hayman DT. Filoviruses in bats: current knowledge and future directions. Viruses 6, 1759-1788, 2014.

67) Olival KJ, Islam A, Yu M, Anthony SJ, Epstein JH, Khan SA, Khan SU, Crameri G, Wang LF, Lipkin WI, Luby SP, Daszak P. Ebola virus antibodies in fruit bats, bangladesh. Emerg Infect Dis 19, 270-273, 2013.

68) Pavlovich SS, Lovett SP, Koroleva G, Guito JC, Arnold CE, Nagle ER, Kulcsar K, Lee A, Thibaud-Nissen F, Hume AJ, Muhlberger E, Uebelhoer LS, Towner JS, Rabadan R, Sanchez-Lockhart M, Kepler TB, Palacios G. The Egyptian Rousette genome reveals unexpected features of bat antiviral immunity. Cell 173, 1098-1110 e1018, 2018.

69) Paweska JT, Jansen van Vuren P, Kemp A, Storm N, Grobbelaar AA, Wiley MR, Palacios G, Markotter W. Marburg virus infection in Egyptian Rousette bats, South Africa, 2013-2014. Emerg Infect Dis 24, 1134-1137, 2018.

70) Pontremoli C, Forni D, Cagliani R, Filippi G, De Gioia L, Pozzoli U, Clerici M, Sironi M. Positive selection drives evolution at the host-filovirus interaction surface. Mol Biol Evol 33, 2836-2847, 2016.

71) R Core Team. R: A Language and Environment for Statistical Computing. R Foundation for Statistical Computing, 2018.

72) Ramirez de Arellano E, Sanchez-Lockhart M, Perteguer MJ, Bartlett M, Ortiz M, Campioli P, Hernandez A, Gonzalez J, Garcia K, Ramos M, Jimenez-Clavero MA, Tenorio A, Sanchez-Seco MP, Gonzalez F, Echevarria JE, Palacios G, Negredo A. First evidence of antibodies against Lloviu virus in Schreiber's bent-winged insectivorous bats demonstrate a wide circulation of the virus in Spain. Viruses 11, 2019.

73) Richter H, Cumming G. First application of satellite telemetry to track African straw‐coloured fruit bat migration. J Zool 275, 172-176, 2008.

74) Roberts B, Eby, P., Tsang, S.M., Sheherazade. *Pteropus alecto* The IUCN Red List of Threatened Species 2017, e.T18715A22080057., 2017.

75) Saeed MF, Kolokoltsov AA, Albrecht T, Davey RA. Cellular entry of Ebola virus involves uptake by a macropinocytosis-like mechanism and subsequent trafficking through early and late endosomes. PLoS Pathog 6, e1001110, 2010.

76) Sarkis S, Lise MC, Darcissac E, Dabo S, Falk M, Chaulet L, Neuveut C, Meurs EF, Lavergne A, Lacoste V. Development of molecular and cellular tools to decipher the type I IFN pathway of the common vampire bat. Dev Comp Immunol 81, 1-7, 2018.

77) Sato M, Maruyama J, Kondoh T, Nao N, Miyamoto H, Takadate Y, Furuyama W, Kajihara M, Ogawa H, Manzoor R, Yoshida R, Igarashi M, Takada A. Generation of bat-derived influenza viruses and their reassortants. Sci Rep 9, 1158, 2019.

78) Swanepoel R, Smit SB, Rollin PE, Formenty P, Leman PA, Kemp A, Burt FJ, Grobbelaar AA, Croft J, Bausch DG, Zeller H, Leirs H, Braack LE, Libande ML, Zaki S, Nichol ST, Ksiazek TG, Paweska JT. Studies of reservoir hosts for Marburg virus. Emerg Infect Dis 13, 1847-1851, 2007.

79) Takada A. Filovirus tropism: cellular molecules for viral entry. Front Microbiol 3, 34, 2012.

80) Takada A, Robison C, Goto H, Sanchez A, Murti KG, Whitt MA, Kawaoka Y. A system for functional analysis of Ebola virus glycoprotein. Proc Natl Acad Sci U S A 94, 14764-14769, 1997.

81) Takadate Y, Kondoh T, Igarashi M, Maruyama J, Manzoor R, Ogawa H, Kajihara M, Furuyama W, Sato M, Miyamoto H, Yoshida R, Hill TE, Freiberg AN, Feldmann H, Marzi A, Takada A. Niemann-Pick C1 heterogeneity of bat cells controls filovirus tropism. Cell Rep, in press

82) Taniguchi S, Watanabe S, Masangkay JS, Omatsu T, Ikegami T, Alviola P, Ueda N, Iha K, Fujii H, Ishii Y, Mizutani T, Fukushi S, Saijo M, Kurane I, Kyuwa S, Akashi H, Yoshikawa Y, Morikawa S. Reston Ebolavirus antibodies in bats, the Philippines. Emerg Infect Dis 17, 1559-1560, 2011.

83) Towner JS, Amman BR, Sealy TK, Carroll SA, Comer JA, Kemp A, Swanepoel R, Paddock CD, Balinandi S, Khristova ML, Formenty PB, Albarino CG, Miller DM, Reed ZD, Kayiwa JT, Mills JN, Cannon DL, Greer PW, Byaruhanga E, Farnon EC, Atimnedi P, Okware S, Katongole-Mbidde E, Downing R, Tappero JW, Zaki SR, Ksiazek TG, Nichol ST, Rollin PE. Isolation of genetically diverse Marburg viruses from Egyptian fruit bats. PLoS Pathog 5, e1000536, 2009.

84) Towner JS, Pourrut X, Albarino CG, Nkogue CN, Bird BH, Grard G, Ksiazek TG, Gonzalez JP, Nichol ST, Leroy EM. Marburg virus infection detected in a common African bat. PLoS One 2, e764, 2007.

85) Vincenot C. *Pteropus dasymallus*, The IUCN Red List of Threatened Species 2017, e.T18722A22080614., 2017.

86) Wang H, Shi Y, Song J, Qi J, Lu G, Yan J, Gao GF. Ebola viral glycoprotein bound to its endosomal receptor Niemann-Pick C1. Cell 164, 258-268, 2016.

87) Yang X-L, Tan CW, Anderson DE, Jiang R-D, Li B, Zhang W, Zhu Y, Lim XF, Zhou P, Liu X-L, Guan W, Zhang L, Li S-Y, Zhang Y-Z, Wang L-F, Shi Z-L. Characterization of a filovirus (Měnglà virus) from *Rousettus* bats in China. Nat Microbiol 4, 390-395, 2019.

88) Yang XL, Zhang YZ, Jiang RD, Guo H, Zhang W, Li B, Wang N, Wang L, Waruhiu C, Zhou JH, Li SY, Daszak P, Wang LF, Shi ZL. Genetically diverse

filoviruses in *Rousettus* and *Eonycteris* spp. bats, China, 2009 and 2015. Emerg Infect Dis 23, 482-486, 2017.

89) Yuan J, Zhang Y, Li J, Zhang Y, Wang LF, Shi Z. Serological evidence of ebolavirus infection in bats, China. Virol J 9, 236, 2012.

90) Zhou P, Tachedjian M, Wynne JW, Boyd V, Cui J, Smith I, Cowled C, Ng JH, Mok L, Michalski WP, Mendenhall IH, Tachedjian G, Wang LF, Baker ML. Contraction of the type I IFN locus and unusual constitutive expression of IFN-alpha in bats. Proc Natl Acad Sci U S A 113, 2696-2701, 2016.